Lawrence Berkeley National Laboratory

Title
On the propagation of a quasi-static disturbance in a heterogeneous, deformable, and porous medium with pressure-dependent properties

Author
Vasco, DW

On the propagation of a quasi-static disturbance in a heterogeneous, deformable, and porous medium with pressure-dependent properties

D. W. Vasco[1]

[1]   Using an asymptotic technique, valid when the medium properties are smoothly varying, I derive a semianalytic expression for the propagation velocity of a quasi-static disturbance traveling within a nonlinear-elastic porous medium. The phase, a function related to the propagation time, depends upon the properties of the medium, including the pressure sensitivities of the medium parameters, and on pressure and displacement amplitude changes. Thus, the propagation velocity of a disturbance depends upon its amplitude, as might be expected for a nonlinear process. As a check, the expression for the phase function is evaluated for a poroelastic medium when the material properties do not depend upon the fluid pressure. In that case, the travel time estimates agree with conventional analytic estimates and with values calculated using a numerical simulator. For a medium with pressure-dependent permeability I find general agreement between the semianalytic estimates and estimates from a numerical simulation. In this case the pressure amplitude changes are obtained from the numerical simulator.

1. Introduction

[2]   Coupled deformation and flow in a porous medium is a topic of great importance. Consequently, it has been the subject of many studies, too numerous to cite here, including the fundamental work of *Biot* [1941, 1956a, 1956b, 1962]. Coupled deformation and flow are also implicit in the early important work in hydrology on the transient pressure variations associated with fluid injection [e.g., *Theis*, 1935; *Jacob and Lohman*, 1952] in the form of a storage coefficient [*de Marsily*, 1986, p. 108]. Unfortunately, modeling deformation and flow in a porous medium is difficult because of the coupling of the fluid and solid and the very different nature of each material. Furthermore, though the fluid can often be modeled as a viscous liquid, the range of behavior of the solid matrix can be significant. A number of investigators have considered poroelastic media, for which the solid component behaves in a linear elastic manner [*Biot*, 1941; *Levy*, 1979; *Burridge and Keller*, 1981; *Segall*, 1985; *Wang*, 2000; *Vasco*, 2009]. However, it is widely recognized that in many situations the material and flow properties may depend upon both the solid deformation and the fluid pressure [*Nelson and Baron*, 1971; *Raghavan et al.*, 1972; *Biot*, 1973; *Samaniego et al.*, 1977; *Walsh and Brace*, 1984; *Gobran et al.*, 1987; *Bethke and Corbet*, 1988; *Goddard*, 1990; *Zimmerman*, 1991; *Wu and Pruess*, 2000; *Bemer et al.*, 2001; *Shapiro*, 2003; *Makse et al.*, 2004; *Murphy et al.*, 2004; *Cappa et al.*, 2006; *Daley et al.*, 2006; *Cheng and Abousleiman*, 2008; *Vasco and Minkoff*, 2009; *Liu et al.*, 2009], resulting in nonlinear governing equations.

[3]   To date, there have been very few analytic or semianalytic studies of such coupled deformation and flow in a medium with pressure-dependent properties. Rather, because of the complexity of the problem, most investigations have utilized numerical methods [*Raghavan et al.*, 1972; *Noorishad et al.*, 1984; *Rutqvist et al.*, 1998]. A handful of analytical studies have focused on the governing equation for fluid pressure with pressure-dependent coefficients [*Wu and Pruess*, 2000; *Murphy et al.*, 2004]. However, these studies do not explicitly include the equation governing displacements in the porous solid, thus neglecting the full coupling of deformation to fluid pressure. In this paper I use an asymptotic technique to derive semianalytic expressions for the displacement of a porous matrix and fluid pressure variations. These expressions may be used, in conjunction with numerical simulation, to gain insight into the propagation of a coupled solid matrix displacement and fluid pressure change. My objective is an expression for the propagation velocity in terms of the parameters of the medium. Such an expression can be used in reservoir characterization, that is, for setting up and solving inverse problems.

[4]   This study links linear poroelasticity to flow in a medium with pressure-dependent properties. I do this by generalizing Biot's equations for a porous medium, allowing for pressure-dependent elastic and flow properties. The work is related to studies in which the diffusion equation governing fluid flow contains pressure-dependent coefficients [*Raghavan et al.*, 1972; *Samaniego et al.*, 1977; *Witherspoon et al.*, 1980; *Wu and Pruess*, 2000; *Vasco and*

---

[1]Earth Sciences Division, Lawrence Berkeley National Laboratory, University of California, Berkeley, California, USA.

Minkoff, 2009]. Here I consider the fully coupled set of equations for deformation and fluid pressure in a medium with pressure-dependent properties. The asymptotic approach developed here is general and applicable to other formulations of the governing equations. The importance of the modeling technique is that it is applicable to coupled nonlinear processes in heterogeneous media [*Vasco*, 2010, 2011].

2. Methodology

[5] In section 2 I present the governing equations for quasi-static flow and displacement in a medium with pressure-dependent properties. Next, an asymptotic methodology is developed in order to estimate the propagation velocity of a coupled fluid and deformation front.

2.1. The Equations Governing Quasi-static Displacement and Flow in a Porous and Deformable Medium

[6] This paper is concerned with the deformation and flow induced by the injection or withdrawal of fluid at depth. I envision a situation in which the fluid pressure undergoes significant change due to injection or withdrawal. The displacement of the solid is driven primarily by the changes in the fluid pressure. Conservation laws provide governing equations for the displacement of the solid matrix $\mathbf{u}(\mathbf{x}, t)$, the displacement of the fluid $\mathbf{w}(\mathbf{x}, t)$ relative to that of the solid, the stress tensor σ, and the fluid pressure P_f [*Noorishad et al.*, 1984; *Wang*, 2000]:

$$\nabla \cdot \boldsymbol{\sigma} = 0, \tag{1}$$

$$\frac{\partial \nabla \cdot \mathbf{w}}{\partial t} + \nabla \cdot \frac{\mu}{k}[\nabla P_f - \rho \mathbf{g}] = 0, \tag{2}$$

where μ is the fluid viscosity, k is the permeability of the porous medium, ρ is the density of the fluid, and $\mathbf{g}$ is the gravitational force vector.

[7] Constitutive laws, relating σ and P_f to $\mathbf{u}$ and $\mathbf{w}$, are required if one is to formulate the governing equations in a solvable form. The fluid is typically modeled as a Newtonian liquid, as discussed by *Bear* [1972]. The flow is usually slow enough that it may considered to be laminar and turbulence may be neglected. As a consequence, one may invoke Darcy's law, relating the fluid pressure gradient to the fluid velocity [*de Marsily*, 1986].

[8] For the porous matrix there are many more choices because of the variability of solid materials. For example, the matrix may consist of a poorly consolidated soil, a porous limestone, or a fractured granitic material. Because I am interested deformation associated with fluid injection over time intervals of seconds to a few months, I will consider the process to be reversible. That is, when the injection is halted, and the fluid pressure returns to its initial value, the deformed body returns to its original configuration. Furthermore, deformation-related changes in material properties, such as the permeability and geomechanical moduli, are also assumed to return to their original values. The most common material model displaying such characteristics is that of a nonlinear-elastic or hyperelastic body [*Ogden*, 1984, p. 206; *Bertram*, 2008, p. 209]. If the solid behaves inelastically, one can consider an incremental

approach, subdividing the time interval of interest into shorter segments over which the deformation is indeed reversible.

[9] In Appendix A I develop constitutive laws for such a nonlinear poroelastic medium. The main results of Appendix A are that I can write the stress tensor σ as

$$\boldsymbol{\sigma} = G\Sigma - \varphi_u \nabla \cdot \mathbf{uI} - \alpha_m P_f \mathbf{I}, \tag{3}$$

where

$$\Sigma = \nabla \mathbf{u} + \nabla \mathbf{u}^T - \frac{2}{3} \nabla \cdot \mathbf{uI} \tag{4}$$

(see equation (A26)). I can relate the divergence of the fluid to the fluid pressure P_f and the divergence of the solid

$$\nabla \cdot \mathbf{w} = -\varphi_m P_f - \alpha_m \nabla \cdot \mathbf{u} \tag{5}$$

(see equation (A27)), and the coefficients G, φ_u, and α_m may depend upon the fluid pressure. Thus, the governing equations (1) and (2) may be written as

$$\nabla \cdot \Sigma + \nabla \zeta \cdot \Sigma - \eta \nabla(\varphi_u \nabla \cdot \mathbf{u} + \alpha P) = 0 \tag{6}$$

$$\frac{\partial(\varphi_m P)}{\partial t} + \frac{\partial(\alpha \nabla \cdot \mathbf{u})}{\partial t} - \nabla \cdot \left[\frac{k}{\mu}(\nabla P + \rho \mathbf{g})\right] = 0, \tag{7}$$

where I have defined the following quantities that depend upon the shear modulus, G,

$$\zeta = -\ln G \tag{8}$$

$$\eta = \frac{1}{G}, \tag{9}$$

and I have dropped the subscript m on α. I emphasize that the coefficients in equations (6) and (7), G, φ_u, α, φ_m, and k may all depend upon the fluid pressure P in addition to any dependence upon the spatial coordinates $\mathbf{x}$. The fluid properties μ and ρ may also depend upon the fluid pressure, while the tensor Σ depends upon spatial coordinates and time. Thus, care must be exercised when taking the derivatives with respect to time and space, because there are implicit dependencies. For example, the spatial derivative of ζ is given by

$$\nabla \zeta = \nabla_x \zeta + \frac{\partial \zeta}{\partial P} \nabla P, \tag{10}$$

where ∇_x signifies that the gradient is applied to the explicit spatial dependence and that P is held fixed. In the expressions that follow I suppress the x subscript on the spatial gradients. Applying the derivative operators to the quantities in parentheses and brackets in equations (6) and (7) results in

$$\nabla \cdot \Sigma + \nabla \zeta \cdot \Sigma + \gamma_p \nabla P \cdot \Sigma - \eta \nabla \varphi_u \nabla \cdot \mathbf{u} - \kappa_u \nabla P \nabla \cdot \mathbf{u}$$
$$- \chi_u \nabla \nabla \cdot \mathbf{u} - \eta \nabla \alpha P - \chi_p \nabla P = 0 \tag{11}$$

$$\alpha_p \frac{\partial P}{\partial t} + \alpha_u \nabla \cdot \mathbf{u} \frac{\partial P}{\partial t} + \alpha \frac{\partial \nabla \cdot \mathbf{u}}{\partial t} - \frac{1}{\mu} \nabla k \cdot \nabla P - \beta_p \nabla P \cdot \nabla P$$

$$-\gamma \nabla P \cdot \mathbf{g} - \frac{1}{\mu} \nabla k \cdot \mathbf{g} - \frac{k}{\mu} \nabla \cdot \nabla P = 0, \tag{12}$$

where

$$\gamma_p = -\frac{\partial \ln G}{\partial P}, \tag{13}$$

$$\kappa_u = \frac{1}{G} \frac{\partial \varphi_u}{\partial P}, \tag{14}$$

$$\chi_u = \frac{1}{G} \varphi_u, \tag{15}$$

$$\chi_p = \frac{1}{G} \left(P \frac{\partial \alpha}{\partial P} + \alpha \right), \tag{16}$$

$$\alpha_p = P \frac{\partial \varphi_m}{\partial P} + \varphi_m, \tag{17}$$

$$\alpha_u = \frac{\partial \alpha}{\partial P}, \tag{18}$$

$$\beta_p = \frac{1}{\mu} \frac{\partial k}{\partial P} + k \frac{\partial \mu^{-1}}{\partial P}, \tag{19}$$

$$\gamma = \frac{k}{\mu} \frac{\partial \rho}{\partial P} + k\rho \frac{\partial \mu^{-1}}{\partial P} + \frac{\rho}{\mu} \frac{\partial k}{\partial P}. \tag{20}$$

In equations (13) through (16) I have used the definitions (8) and (9) to make the dependence upon the shear modulus, G, explicit.

2.2. An Asymptotic Expression for the Propagation Velocity

[10] In Appendix B I apply the method of multiple scales, an asymptotic technique [*Whitham*, 1974; *Anile et al.*, 1993], to the governing equations (11) and (12). The goal is a semi-analytic expression for the propagation velocity of a disturbance in terms of the medium parameters. The principle underlying the method of multiple scales is that the properties of the medium vary smoothly in space. That is, away from interfaces and boundaries, such as faults, the elastic and flow properties of the medium are smoothly varying. This assumption is compatible with one of my intended applications, the solution of inverse problems and efficient imaging of properties within the Earth. For such applications, because of the sparsity of data, one must often assume that only the smoothly varying component of a heterogeneous distribution of properties may be determined.

[11] The measure of smoothness is with respect to the scale length of the disturbance. That is, the propagating disturbance has an associated length scale, the distance over which the displacement and pressure fields change from their background values to new values behind the propagating front. I denote the length scale of the propagating disturbance

by l and the length scale of the heterogeneity by L. The smoothness of the heterogeneity with respect to the length scale of the propagating disturbance means that $l \ll L$. One can define a parameter characterizing the smoothness of the medium in terms of the ratio of the scale lengths:

$$\varepsilon = \frac{l}{L}. \tag{21}$$

I can define an alternative coordinate system, the "slow" coordinates, in terms of ε [*Anile et al.*, 1993]:

$$\mathbf{X} = \varepsilon \mathbf{x}, \tag{22}$$

$$T = \varepsilon t. \tag{23}$$

Quantities associated with a propagating disturbance, such as the amplitude of the disturbance, and the travel time of the disturbance are best described as functions of the slow coordinates. These two quantities, the travel time and the amplitude of the disturbance, are two of the most important aspects of a propagating disturbance. They can provide important information related to the properties of a porous medium. For example, the travel time of a deformation front induced by fluid production can be used to image the flow properties of a reservoir, in the manner of geophysical tomography [*Rucci et al.*, 2010].

[12] An asymptotic solution may be constructed in terms of the ratio of the scale lengths, specifically as a power series in ε. For example, I can represent the fluid pressure as

$$P(\mathbf{X}, T, \theta_p) = P_b(\mathbf{X}, T) + \int_0^T e^{\theta_p(\mathbf{X},\tau)} \sum_{i=0}^{\infty} \varepsilon^i P_i(\mathbf{X}, \tau) d\tau. \tag{24}$$

This representation, in terms of an integral over time, is appropriate for a step function source in time, and produces a monotonic increase or decrease in pressure. The function $\theta_p(\mathbf{X}, T)$ is the phase associated with the transient pressure disturbance, a quantity related to the propagation time. The functions $P_i(\mathbf{X}, T)$ are the amplitude functions, representing the base amplitude of the disturbance $P_0(\mathbf{X}, T)$ and subsequent, higher-order corrections. The displacement of the solid matrix (**u**) has a similar series representation for a step function source. For an impulsive source, such as a delta function, one can use the more conventional representation

$$P(\mathbf{X}, T, \theta_p) = P_b(\mathbf{X}, T) + e^{\theta_p(\mathbf{X},\tau)} \sum_{i=0}^{\infty} \varepsilon^i P_i(\mathbf{X}, \tau) \tag{25}$$

found in texts on high-frequency asymptotic solutions [*Kline and Kay*, 1965, p. 284; *Anile et al.*, 1993, p. 54].

[13] I can write the governing equations (11) and (12) in terms of the slow coordinates. In the new coordinate system the differential operators are also transformed. In addition, the derivative operators need to account for the implicit dependence of $P(\mathbf{X}, T, \theta_p)$ on $\theta_p(\mathbf{X}, T)$. Thus, for example the time derivative becomes

$$\frac{\partial P}{\partial t} = \varepsilon \frac{\partial P}{\partial T} + \frac{\partial \theta_p}{\partial t} \frac{\partial P}{\partial \theta_p}, \tag{26}$$

while the spatial derivatives, such as those of $\mathbf{u}$, are modified as

$$\frac{\partial \mathbf{u}}{\partial x_i} = \varepsilon \frac{\partial \mathbf{u}}{\partial X_i} + \frac{\partial \theta}{\partial x_i} \frac{\partial \mathbf{u}}{\partial \theta}. \qquad (27)$$

In Appendix B I transform the governing equations (11) and (12) into the slow coordinate system. Because it is assumed that the heterogeneity is smoothly varying, ε is small, and only terms of lowest order, order $\varepsilon^0 \sim 1$, are retained, resulting in the two equations:

$$\left[s^2 \bar{\mathbf{U}} + \frac{1}{3}(\mathbf{s} \cdot \bar{\mathbf{U}})\mathbf{s} \right] + \gamma_p \bar{P} \left[\mathbf{p} \cdot \mathbf{s}\bar{\mathbf{U}} + (\mathbf{p} \cdot \bar{\mathbf{U}})\mathbf{s} - \frac{2}{3}(\mathbf{s} \cdot \bar{\mathbf{U}})\mathbf{p} \right] \qquad (28)$$
$$- \kappa_u \bar{P}(\mathbf{s} \cdot \bar{\mathbf{U}})\mathbf{p} - \chi_u(\mathbf{s} \cdot \bar{\mathbf{U}})\mathbf{s} - \chi_p \bar{P}\mathbf{p} = 0,$$

$$\alpha_p \frac{\partial \theta_p}{\partial t} \bar{P} + \alpha_u \frac{\partial \theta_p}{\partial t} \mathbf{s} \cdot \bar{\mathbf{U}}\bar{P} + \alpha \frac{\partial \theta_u}{\partial t} \mathbf{s} \cdot \bar{\mathbf{U}} - \beta_p p^2 \bar{P}^2 \qquad (29)$$
$$- \gamma \mathbf{p} \cdot \mathbf{g}\bar{P} - \frac{k}{\mu} p^2 \bar{P} = 0,$$

where $\mathbf{p}$ and $\mathbf{s}$ are the phase gradient vectors,

$$\mathbf{p} = \nabla \theta_p, \qquad (30)$$

$$\mathbf{s} = \nabla \theta_u, \qquad (31)$$

and $p = |\nabla \theta_p|$ and $s = |\nabla \theta_s|$.

[14] Furthermore, because of the specific form chosen for the asymptotic expansion, equation (25), and its equivalent for $\mathbf{u}(\mathbf{X}, T, \theta_u)$, the partial derivatives with respect to θ are given by

$$\frac{\partial P}{\partial \theta_p} = P - P_b = \bar{P}, \qquad (32)$$

and similarly for $\mathbf{u}$,

$$\frac{\partial \mathbf{u}}{\partial \theta_u} = \mathbf{u} - \mathbf{u}_b = \bar{\mathbf{U}}. \qquad (33)$$

[15] Equations (28) and (29) are two equations constraining the properties of the propagating pressure and deformation disturbances. For example, the equations constrain the pressure and displacement amplitude changes with respect to the background values, given by $\bar{P}$ and $\bar{\mathbf{U}}$. The phase variables θ_p and θ_u, or rather the derivatives of the phase variables, are also contained in equations (28) and (29). Thus, there are more unknowns than constraints in the two equations. In order to make progress I must provide additional assumptions or a means for computing some of these unknowns. One assumption that will be invoked is that the deformation and pressure fronts are coupled. That is, I will assume that a rapid change in fluid pressure is accompanied by the initiation of matrix deformation, so that $\theta_p = \theta_u$. Note that the time variation following the initiation can differ for the pressure and displacement, depending upon the time variation of the amplitude functions $P_i(\mathbf{X}, T)$ and

$\mathbf{u}_i(\mathbf{X}, T)$. If $\theta_p = \theta_u$ then $\mathbf{p} = \mathbf{s}$ and equations (28) and (29) reduce to

$$p^2(1 + \gamma_p \bar{P})\bar{\mathbf{U}} + (\Upsilon \mathbf{p} \cdot \bar{\mathbf{U}} - \chi_p \bar{P})\mathbf{p} = 0, \qquad (34)$$

$$[\alpha_p \bar{P} + \Psi \mathbf{p} \cdot \bar{\mathbf{U}}]\frac{\partial \theta}{\partial t} - \gamma \bar{P}\mathbf{p} \cdot \mathbf{g} - \left(\beta_p \bar{P} + \frac{k}{\mu} \right)\bar{P}p^2 = 0, \qquad (35)$$

where

$$\Upsilon = \frac{1}{3} + \frac{1}{3}\gamma_p \bar{P} - \kappa_u \bar{P} - \chi_u, \qquad (36)$$

$$\Psi = \alpha_u \bar{P} + \alpha, \qquad (37)$$

and θ denotes the common value of θ_p and θ_u. Because $\mathbf{p} = \nabla \theta$, the two equations may be thought of as differential equations for θ, given the amplitude functions $\bar{P}$ and $\bar{\mathbf{U}}$.

[16] Equations (34) and (35) constrain the amplitude variations $\bar{P}$ and $\bar{\mathbf{U}}$ which are also unknown. In particular, these two equations are polynomials in the amplitude terms. The polynomial dependence on the amplitudes is a generalization of the linear dependence that appears in physical problems in which the governing equations are linear. For linear systems, one uses the condition that the governing equations has a nontrivial solution to derive a single, nonlinear partial differential equation for θ, the eikonal equation [*Karal and Keller*, 1959; *Kravtsov and Orlov*, 1990]. The condition is a well known theorem in linear algebra: for a nontrivial solution of a homogeneous system of equation to exist the determinant of the matrix of coefficients must vanish [*Noble and Daniel*, 1977]. It may be possible to generalize this approach to the polynomial equations (34) and (35), because there are equivalent conditions for a polynomial system to have a nontrivial solution [*Cox et al.*, 1998; *Sturmfels*, 2002]. This condition is given by the vanishing of the resultant which is the determinant of a matrix whose entries are the coefficients of the equations and powers of one of the variables, either $\bar{P}$ or $\bar{U}$. An alternative approach to the method of resultants would be to find the amplitude terms $\bar{P}$ and $\bar{\mathbf{U}}$ in some fashion. For example, the amplitude functions could be specified by the output of a numerical simulator, then equations (34) and (35) would constrain the phase of the propagating front, θ.

[17] In considering equations (34) and (35) one must be mindful that the coefficients are generally pressure dependent, representing nonlinear functions of pressure that also vary spatially. In this work I am interested in the propagation of a coupled deformation and pressure front, in particular the propagation velocity and its relationship to the properties of the medium. The propagation velocity, and the related quantity the phase θ, are determined by the movement of the leading edge of the front. Because the leading edge of the front encroaches upon material in the background state, with pressure P_b and displacement $\mathbf{u}_b$ (typically taken to be zero), one would expect that the coefficients reflect such conditions. That is, the velocity of the leading edge of the propagating front is primarily influenced by the background conditions. As in the work of *Anile et al.* [1993], a more formal mathematical approach may be taken on the basis of an expansion of the coefficients in powers of

ε. This expansion follows from the representation of the pressure as an asymptotic series in ε (see equation (25)). Consider, for example, $\chi_p(\mathbf{X}, P)$, which may be expanded as

$$\chi_p(\mathbf{X}, P) = \chi_p(\mathbf{X}, P_b + \bar{P}_0) + \varepsilon \frac{\partial \chi_p}{\partial P}(\mathbf{X}, P_b + \bar{P}_0) + O(\varepsilon^2), \tag{38}$$

where

$$\bar{P}_0(\mathbf{X}, T) = \int_0^T e^{\theta(\mathbf{X}, \tau)} P_0(\mathbf{X}, \tau) d\tau \tag{39}$$

in the case of a step function source or by the time derivative of (39) for an impulsive source time function. To order ε one finds that $\chi_p(\mathbf{X}, P) = \chi_p(\mathbf{X}, P_b + \bar{P}_0)$. The moment at which the coupled front arrives at an observation point $\mathbf{X}$, which I denote by T_{arrival}, the quantity $\bar{P}_0(\mathbf{x}, T_{\text{arrival}})$ is zero and hence $\chi_p(\mathbf{X}, P) = \chi_p(\mathbf{X}, P_b)$.

[18] A cursory examination of equations (34) and (35) indicates that there are two orientations of the solid displacement vector $\bar{\mathbf{U}}$ that are important. The significance of the orientations is due to the presence of terms containing $\mathbf{p} \cdot \bar{\mathbf{U}}$ in these two equations. In particular, the displacement $\bar{U}$ can be either perpendicular to the direction of propagation, $\mathbf{p}$, or parallel to it. These two cases are similar to those identified in the study of linear poroelastic media [*Pride*, 2005] I shall examine each of these possibilities in succession.

2.2.1. Transverse Displacement

[19] First consider transverse displacement, such as the displacement associated with a shear wave. When $\mathbf{p}$ is perpendicular to $\bar{\mathbf{U}}$ the two equations (34) and (35) decouple. If $\mathbf{p}$ is perpendicular to $\bar{\mathbf{U}}$ then equation (34) implies two conditions,

$$p^2(1 + \gamma_p \bar{P})\bar{\mathbf{U}} = 0 \tag{40}$$

$$\chi_p \bar{P} \mathbf{p} = 0,$$

because the vectors $\bar{\mathbf{U}}$ and $\mathbf{p}$ are orthogonal for transverse motion. From the second condition one finds that if χ_p is not zero (the equations are coupled; see the definition of χ_p, equation (16)) then either $\mathbf{p} = 0$ or $\bar{P} = 0$. From equation (40), with $\bar{P}$ equal to zero, one finds that either $\bar{\mathbf{U}}$ vanishes or the slowness p vanishes. If $\bar{\mathbf{U}}$ vanishes then one has the trivial solution in which there is no disturbance. If $\bar{\mathbf{U}}$ is nonzero but p vanishes then $|\nabla p| = p = 0$ and the phase is constant in space. If the phase is constant then the travel time, a function of the phase, is also constant over the medium and the transverse displacement propagates infinitely fast. Note that $p = 0$ is compatible with equation (35) if it corresponds to $\theta = 0$. As indicated by *Vasco* [2008, 2009], the infinite velocity of a transverse displacement is a consequence of the quasi-static approximation.

2.2.2. Longitudinal Displacement

[20] Now consider the more interesting case of longitudinal displacement, in which the displacement of the solid,

$\bar{\mathbf{U}}$, is oriented along the direction of propagation, $\mathbf{p}$. In this case I can write the solid displacement in the form

$$\bar{\mathbf{U}}(\mathbf{X}, T) = \bar{U}(\mathbf{X}, T)\mathbf{p} \tag{41}$$

where $\bar{U}(\mathbf{X}, T)$ is the amplitude. Substituting this expression into equations (34) and (35) and evaluating the scalar products gives

$$[p^2(1 + \gamma_p \bar{P})\bar{U} + \Upsilon p^2 \bar{U} - \chi_p \bar{P}]\mathbf{p} = 0, \tag{42}$$

$$[\alpha_p \bar{P} + \Psi p^2 \bar{U}]\frac{\partial \theta}{\partial t} - \gamma \bar{P} \mathbf{p} \cdot \mathbf{g} - \left(\beta_p \bar{P} + \frac{k}{\mu}\right)p^2 \bar{P} = 0. \tag{43}$$

For a phase gradient vector, $\mathbf{p}$, that does not vanish, the quantity in brackets in equation (42) must equal zero in order for the equation to be satisfied. Two coupled scalar equations, relating $\bar{U}$, $\bar{P}$, and $\mathbf{p}$, result:

$$p^2 \gamma_p \bar{P} \bar{U} + (1 + \Upsilon)p^2 \bar{U} - \chi_p \bar{P} = 0, \tag{44}$$

$$[\alpha_p \bar{P} + \Psi p^2 \bar{U}]\frac{\partial \theta}{\partial t} - \gamma \bar{P} \mathbf{p} \cdot \mathbf{g} - \left(\beta_p \bar{P} + \frac{k}{\mu}\right)p^2 \bar{P} = 0. \tag{45}$$

The coefficients are defined in terms of the geomechanical and flow properties of the medium at the background pressure P_b. Substituting for Υ and Ψ, from definitions (36) and (37), respectively, I can write equations (44) and (45) as

$$\left(\frac{4}{3}\gamma_p - \kappa_u\right)p^2 \bar{P} \bar{U} + \left(\frac{4}{3} - \chi_u\right)p^2 \bar{U} - \chi_p \bar{P} = 0 \tag{46}$$

$$[\alpha_u p^2 \bar{P} \bar{U} + \alpha_p \bar{P} + \alpha p^2 \bar{U}]\frac{\partial \theta}{\partial t} - \gamma \bar{P} \mathbf{p} \cdot \mathbf{g} - \left(\beta_p \bar{P} + \frac{k}{\mu}\right)p^2 \bar{P} = 0. \tag{47}$$

When considered as equations in $\bar{P}$ and $\bar{U}$, equations (46) and (47) constitute two quadratic equations.

2.2.2.1. Full Pressure Sensitivity

[21] The coefficients γ_p and κ_u are determined by the pressure sensitivity of the shear modulus G (see equations (13) and (14)) and the elastic modulus φ_u, respectively. If the coefficients γ_p and κ_u, are not both zero, I can eliminate the product term $\bar{P}\bar{U}$ in equations (46) and (47). Specifically, I can solve equation (46) for the nonlinear term, $p^2 \bar{P} \bar{U}$, a term that also appears in equation (47). Substituting the resulting expression into equation (47) results in a quadratic equation for p:

$$p^2 + \Gamma \mathbf{p} \cdot \mathbf{g} - \Omega \frac{\partial \theta}{\partial t} = 0, \tag{48}$$

where I have defined the coefficients

$$\Gamma = \frac{\gamma}{\beta_p \bar{P} + k\mu^{-1}} \tag{49}$$

$$\Omega = \frac{\Omega_p \bar{P} + \Omega_u p^2 \bar{U}}{(\beta_p \bar{P} + k\mu^{-1})\bar{P}}. \tag{50}$$

The parameters Ω_p and Ω_u in equation (50) are defined in terms of the poroelastic properties of the medium and their pressure sensitivity:

$$\Omega_p = \alpha_p + \frac{\alpha_u \chi_p}{\frac{4}{3}\gamma_p - \kappa_u} \qquad (51)$$

$$\Omega_u = \alpha + \frac{\alpha_u\left(\chi_u - \frac{4}{3}\right)}{\frac{4}{3}\gamma_p - \kappa_u}. \qquad (52)$$

2.2.2.2. Partial Pressure Sensitivity

[22] Now consider the case in which there is only a partial sensitivity to fluid pressure, that is, the geomechanical properties G and φ_u do not depend upon the fluid pressure. This situation is similar to that studied by *Wu and Pruess* [2000] and *Murphy et al.* [2004], where the governing equation for fluid pressure is generalized to allow for pressure-dependent coefficients. Then the product term $\bar{P}\bar{U}$ in equation (46) vanishes. In addition, because α_u measures the sensitivity of α to changes in fluid pressure (see equation (18)), the product term $\bar{P}\bar{U}$ in equation (47) also vanishes. Using the reduced equation (46) I can solve for $p^2\bar{U}$ in terms of $\bar{P}$. Substituting this expression for $p^2\bar{U}$ into equation (47) gives

$$\left(\beta_p\bar{P} + \frac{k}{\mu}\right)p^2 + \gamma\mathbf{p}\cdot\mathbf{g} - \left(\alpha_p + \frac{\alpha\chi_p}{\frac{4}{3} - \chi_u}\right)\frac{\partial\theta}{\partial t} = 0, \qquad (53)$$

after canceling the common factor $\bar{P}$. This equation may also be written as a quadratic equation in p:

$$p^2 + \Gamma\mathbf{p}\cdot\mathbf{g} - \Omega_v\frac{\partial\theta}{\partial t} = 0, \qquad (54)$$

where Γ is given above (equation (49)) and

$$\Omega_v = \left(\beta_p\bar{P} + \frac{k}{\mu}\right)^{-1}\left[\alpha_p + \frac{\alpha\chi_p}{\frac{4}{3} - \chi_u}\right]. \qquad (55)$$

[23] Equation (54) is an equation in the components of $\mathbf{p}$ and θ. Because $\mathbf{p} = \nabla\theta$, the equation is a nonlinear partial differential equation for θ, reminiscent of the eikonal equation [*Kline and Kay*, 1965; *Sethian*, 1999]. The equation is a scalar differential equation, hence it is much easier to solve then is the full coupled system, composed of equations (11) and (12). However, because of the presence of the amplitude term $\bar{P}$, one must still solve the governing equations using a numerical simulator. The main point is that one can obtain θ for a little additional effort. Furthermore, the terms in equation (54) provide insight into the properties that determine the propagation velocity of the coupled deformation and pressure front.

2.3. The Computation of the Phase Function

[24] Equation (48) is explicit equation for the phase function $\theta(\mathbf{x}, t)$ which may be written as

$$\nabla\theta \cdot \nabla\theta + \Gamma\nabla\theta \cdot \mathbf{g} - \Omega\frac{\partial\theta}{\partial t} = 0, \qquad (56)$$

where I have substituted the gradient of the phase (θ) for the vector $\mathbf{p}$. Equation (56) is a first-order, nonlinear, scalar partial differential equation for $\theta(\mathbf{x}, t)$. Such equations are

rather common in physical applications and mathematical physics [*Lanczos*, 1986, p. 229] and there are well developed techniques for their solution [*Courant and Hilbert*, 1962; *Sneddon*, 2006]. For example, there are now efficient numerical schemes, primarily finite differences, developed for hyperbolic conservation laws [*LeVeque*, 1992; *Crandall and Lions*, 1983; *Crandall et al.*, 1984; *Sethian*, 1999]. The techniques have been generalized to problems in which the propagation speed depends upon the direction of propagation [*Sethian and Strain*, 1992; *Lecomte*, 1993; *Eaton*, 1993; *Soukina et al.*, 2003].

[25] There are also well-established techniques that are efficient and provide additional insight, the method of characteristics [*Courant and Hilbert*, 1962]. In the method of characteristics, the solutions are defined along trajectories through the model. Each trajectory represents a propagation path through the medium and indicates those parts of the model influencing a given observation. As indicted by *Vasco et al.* [2000] and *Vasco and Finsterle* [2004], the trajectories may be used, in the manner of ray theory, to compute model parameter sensitivities required by many inversion algorithms [*Menke*, 1984]. Ray-based sensitivities form the basis for very efficient tomographic imaging methods [*Iyer and Hirahara*, 1993]. The trajectories are also useful in interpreting observed waveforms, particularly in decomposing multiple arrivals in terms of component pulses that travel along different paths [*Vasco et al.*, 2003].

3. Applications

[26] In section 3 I will illustrate the concepts and equations presented in section 2. First, as a reference case, I discuss transient propagation in a poroelastic solid where both the medium and fluid properties are independent of the fluid pressure. This will allow for a comparison between travel time estimates provided by the asymptotic approach and analytic and numeric predictions. Furthermore, it will provide a connection to previous work on quasi-static and broadband propagation in a poroelastic medium [*Vasco*, 2008, 2009]. Next, I consider transient propagation in a medium in which the flow properties depend upon the fluid pressure while the geomechanical properties do not. In particular, I examine the case in which only the permeability depends upon the fluid pressure. Thus, I shall begin with equation (54), corresponding to the case of partial sensitivity to fluid pressure.

3.1. Poroelastic Propagation

[27] As a starting point, consider the propagation of a coupled disturbance in a linear poroelastic medium. In a linear poroelastic medium the coefficients are insensitive to changes in fluid pressure. Thus, the coupling coefficients related to the pressure sensitivity of the medium, specifically γ_p, κ_u, α_u, β_p and γ in equations (11) and (12) vanish (see equations (13)–(20)) and the equations reduce to

$$\nabla\cdot\Sigma + \nabla\zeta\cdot\Sigma - \eta\nabla\varphi_u\nabla\cdot\mathbf{u} - \chi_u\nabla\nabla\cdot\mathbf{u} - \eta\nabla\alpha P - \chi_p\nabla P = 0 \qquad (57)$$

$$\alpha_p\frac{\partial P}{\partial t} + \alpha\frac{\partial\nabla\cdot\mathbf{u}}{\partial t} - \frac{1}{\mu}\nabla k\cdot\nabla P$$

$$-\gamma\nabla P\cdot\mathbf{g} - \frac{1}{\mu}\nabla k\cdot\mathbf{g} - \frac{k}{\mu}\nabla\cdot\nabla P = 0. \qquad (58)$$

As is evident in equations (57) and (58), the fluid pressure and the matrix displacements are linked in a poroelastic medium through linear coupling terms [*Wang*, 2000].

[28] Now consider equation (53), which governs the evolution of the phase. Because the properties of the medium do not vary with pressure, I consider the expression (55) with $\beta_p = 0$,

$$\Omega_v = \left(\frac{k}{\mu}\right)^{-1}\left[\alpha_p + \frac{\alpha\chi_p}{\frac{4}{3} - \chi_u}\right]. \tag{59}$$

Using the fact that $\alpha_p = \varphi_m$, $\chi_p = \alpha/G$, $\chi_u = \varphi_u/G$ (see equations (17), (16), and (15)), I can write Ω_v as

$$\Omega_v = \left(\frac{k}{\mu}\right)^{-1}\left[\varphi_m + \frac{\alpha^2}{\frac{4}{3}G - \varphi_u}\right]. \tag{60}$$

Using the relationships between φ_m and φ_u and the undrained bulk modulus, K_u, Biot's C modulus, C, and the fluid storage coefficient M discussed in Appendix A (see equations (A32) and (A36)), I can write equation (60) as

$$\Omega_v = \left(\frac{k}{\mu}\right)^{-1}\left[\frac{1}{M} + \frac{\alpha^2}{\frac{4}{3}G + K_u - \frac{C^2}{M}}\right] \tag{61}$$

or

$$\Omega_v = \left(\frac{k}{\mu}\right)^{-1}\left[\frac{1}{M} + \frac{\alpha^2}{H - \frac{C^2}{M}}\right] \tag{62}$$

if I define the undrained *P* wave modulus

$$H = K_u + \frac{4}{3}G \tag{63}$$

as done by *Pride* [2005]. Expression (62) is similar to that by *Vasco* [2008] if one accounts for the differences in the variable names due to a slightly different formulation. As in that paper, the expression Ω_v may be interpreted as the sum of a slowness contribution due to diffusion in the fluid and a correction due to the poroelastic medium. Factoring out $1/M$ and rearranging terms, I can write equation (62) as

$$\Omega_v = \left(\frac{k}{\mu}\right)^{-1}\frac{1}{M}\left[\frac{H - \frac{C^2}{M} + M\alpha^2}{H - \frac{C^2}{M}}\right]. \tag{64}$$

Using the fact that $\alpha = \alpha_m = C/M$ (see equation (A33)), I can write equation (64) as

$$\Omega_v = \left(\frac{k}{\mu}\right)^{-1}\frac{1}{M}\left[\frac{H}{H - \frac{C^2}{M}}\right], \tag{65}$$

which is identical to the expression for the Biot slow wave, given in the study of *Pride* [2005]. Therefore, in the case of a poroelastic medium, the expression for Ω_v reduces to existing expressions for the slowness of a propagating disturbance.

[29] Next, I will derive a low-order solution for a disturbance propagating in a poroelastic medium. To keep things simple I shall neglect gravitational effects. If gravitational effects can be omitted, I can substitute either expression (62), or the equivalent expression (65), into equation (54) which reduces to a first-order, nonlinear partial differential equation for θ,

$$\nabla\theta \cdot \nabla\theta - \Omega_v \frac{\partial\theta}{\partial t} = 0. \tag{66}$$

In equation (66) I have used the fact that $\mathbf{p} = \nabla\theta$, as in equation (30). In section 3.1 I shall assume that the permeability does not depend upon time. Then, I can use the separation of variables to determine the space and time dependence. Specifically, I assume a separable form for the phase function [*Vasco*, 2011]

$$\theta(\mathbf{x}, t) = \beta(t)\sigma^2(\mathbf{x}). \tag{67}$$

As shown by *Vasco* [2011], the time dependence is given by

$$\beta(t) = -\frac{1}{4t}.$$

Following *Vasco* [2008, 2011], I can use the well-known [*Kline and Kay*, 1965; *Cerveny* 1972; *Kravtsov and Orlov*, 1990] method of characteristics [*Courant and Hilbert*, 1962] to determine the spatial dependence of the solution, $\sigma(\mathbf{x})$. In particular, I can rewrite the equation for the function $\sigma(\mathbf{x})$, which is the eikonal equation, in ray coordinates as

$$\frac{d\sigma}{dr} = \sqrt{\Omega_v}$$

where r is a parameter signifying the distance along the trajectory or raypath. Integrating along the trajectory, $\mathbf{x}(r)$, results in the expression

$$\sigma(\mathbf{x}(r)) = \int_{\mathbf{x}(r)}\sqrt{\Omega_v}dr \tag{68}$$

for the function σ. Thus, from equation (67)

$$\theta(\mathbf{x}, t) = -\frac{\sigma^2(\mathbf{x})}{4t} \tag{69}$$

where $\sigma(\mathbf{x})$ is given by equation (68)

[30] Using equation (69) and the asymptotic series associated with an impulsive source, equation (25), I can write the zeroth-order solution for the pressure as

$$P(\mathbf{X}, t, \theta) = P_b(\mathbf{X}, t) + e^{\theta(\mathbf{X},t)}P_0(\mathbf{X}, t). \tag{70}$$

Using the solution obtained by the separation of variables [*Vasco*, 2010, 2011], I can write the solution as

$$P(\mathbf{X}, t, \sigma) = P_b(\mathbf{X}, t) + \frac{\sigma}{2\sqrt{\pi t^3}}e^{-\sigma^2/4t} * P_0(\mathbf{X}, t). \tag{71}$$
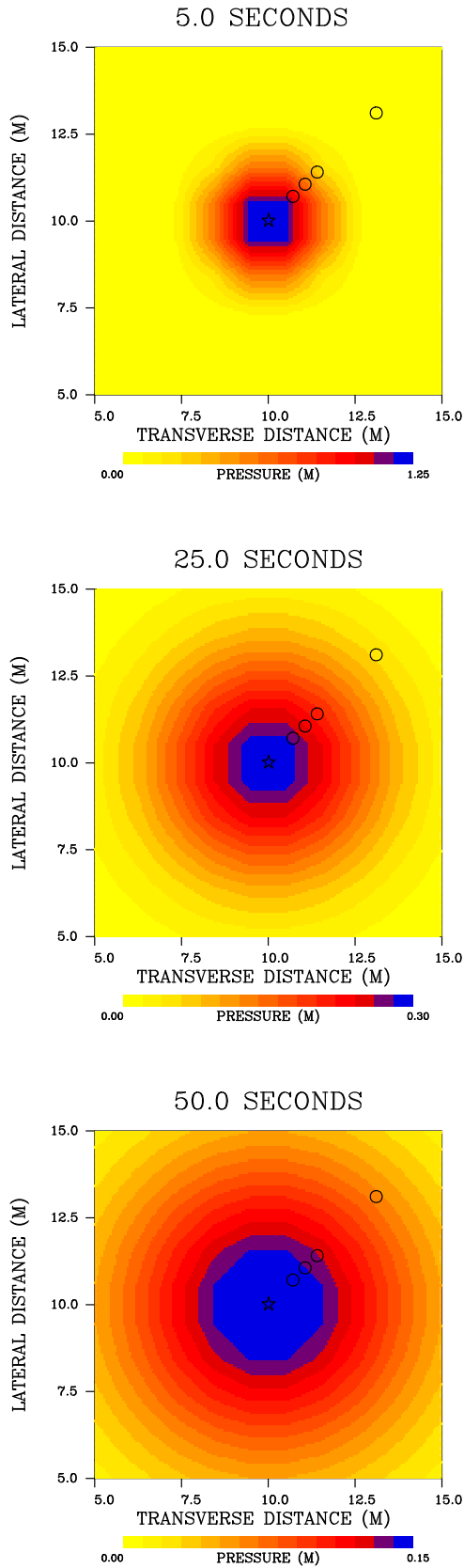
Figure 1

where the asterisk signifies a convolution in time, and

$$\sigma(\mathbf{x}(r)) = \int_{\mathbf{x}(r)} \sqrt{\Omega_v} dr \qquad (72)$$

The amplitude function $P_0(\mathbf{X}, t)$, obtained by considering terms of order ε in the asymptotic expansion, is given by *Vasco* [2008]. In many cases the function $P_0(\mathbf{X}, t)$ can be partitioned into a source time function [*Bracewell*, 1978] determined by the injection rate, $S(t)$, and an spatially dependent term, giving the form

$$P(\mathbf{X}, t, \theta) = P_b(\mathbf{X}, t) + \frac{\sigma}{2\sqrt{\pi t^3}} e^{-\sigma^2/4t} * S(t) P_0(\mathbf{X}). \qquad (73)$$

[31] For an impulsive source, represented by a delta function $\delta(t)$, one can relate the function $\sigma(\mathbf{x}(r))$ to the arrival time of the peak pressure, as noted by *Virieux et al.* [1994] and *Vasco et al.* [2000]. The peak of the pressure curve coincides with the vanishing of the time derivative of $P(\mathbf{X}, t, \theta)$ given by equation (73). This condition gives

$$\frac{\partial P(\mathbf{X}, t, \sigma)}{\partial t} = \frac{1}{t}\frac{3}{2} - \frac{1}{t^2}\frac{\sigma^2}{4} = 0, \qquad (74)$$

which implies that

$$\sqrt{T_{\text{peak}}} = \frac{\sigma}{\sqrt{6}} = \frac{1}{\sqrt{6}} \int_{\mathbf{x}(r)} \sqrt{\Omega_v} dr, \qquad (75)$$

where T_{peak} is the arrival time of the peak pressure. Thus, one can relate σ to the time of arrival of the peak pressure at a particular location. Furthermore, this arrival time can be related to the poroelastic properties of the medium, through Ω_v which is given by the expression (65).

[32] In order to validate the travel time estimate I compare it to the results from a numerical simulation. The numerical simulation can also help one to visualize the time and space variation of the fluid pressure. In Figure 1 I plot three pressure snapshots from a numerical simulation in which fluid is injected into a central well. The simulation is conducted using the finite element code TOCHNOG [*Roddeman*, 2001] which can model coupled fluid flow and solid deformation. As shown below, TOCHNOG can also model coupled deformation and flow in a medium with pressure-dependent properties. The pressure evolution in the numerical simulation results plotted in Figure 1 is dominated by the changes near the injection well. The pressure changes gradually diffuse away from the injection well and it is difficult to define either a propagating front or a travel time.

[33] The difficulties in trying to capture diffusive propagation become clearer if one plots the time variation of the pressure calculated for a sequence of observation points

Figure 1. Simulated pressures at three times (5.0, 25.0, and 50.0 s) for fluid injection into a poroelastic medium. The scale indicates pressure deviations from the background value. The injection well is indicated by the open star at the center of the simulation grid. Only the central portion of the grid is shown. The four open circles indicate points at which pressure time series were extracted.

located progressively farther from the injection well. Four such observation points are indicated by the open circles in Figure 1. The simulated transient pressure at each of the four wells is shown in Figure 2. Note how the pressure at each well initially increases, reaching a peak, and then slowly decays with time. Thus, for the impulsive source used in the simulation there is indeed a peak pressure, and a peak pressure arrival time at each observation point. The difficulty in trying to capture the spatial evolution of this transient feature, as in Figure 1, is due to the fact that the pressure decreases dramatically with distance from the well. Thus, at all times, the pressure variations are dominated by changes near the injection well, as is apparent in Figure 1.

[34] One way to reduce the dominance of the changes near the injection well is to normalize all the pressure changes in each grid block by the peak pressure observed in that grid block. Thus, when the changes plotted in Figure 2 are normalized by their peak values, one obtains the time variations shown in Figure 3. Now the pressure variations near the injection well no longer dominate. In Figure 4 I plot the normalized pressure changes for the three snapshots that were shown previously in Figure 1. The normalized pressure displays the transient propagation noted above and one can clearly define an arrival time for each point on the simulation grid. For each element of the simulation grid there will be a pressure time series, similar to those shown in Figure 3. By estimating the peak pressure and the time at which the peak pressure is attained, one can determine an arrival time. Figure 5 is a plot of the estimated arrival times for the simulation shown in Figure 1. Note how, unlike propagation of a nondispersive wave, the speed of the disturbance changes with distance from the injection source.

[35] Using the asymptotic travel time estimate, provided by equation (75), I can predict the arrival time of the peak pressure. The expression for Ω_v, equation (65) may be used
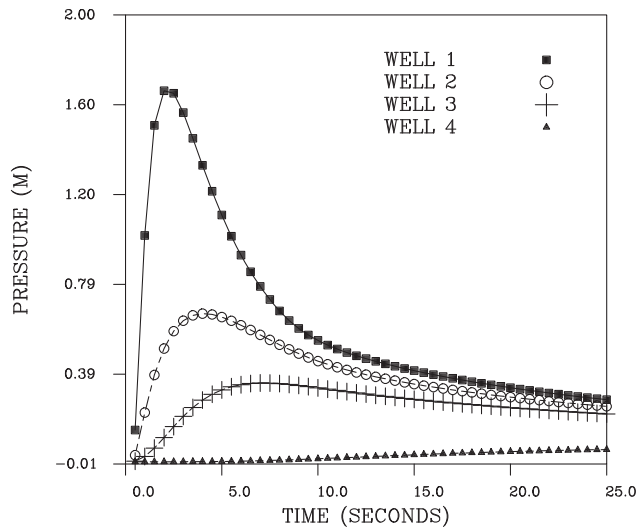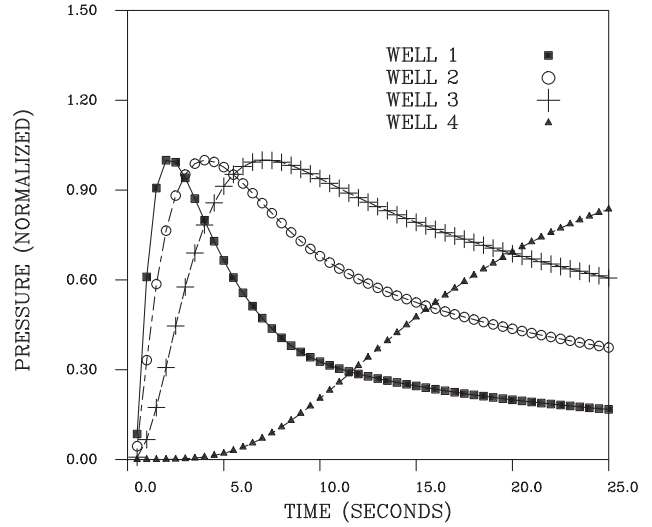
Figure 3.   Normalized transient pressure variations for the four points on the simulation grid shown in Figure 1. That is, these are the curves shown in Figure 2, normalized by their peak values.

to relate the arrival time to the properties of the porous medium. Note that, for a homogeneous porous medium in which the pressure effects dominate the matrix displacements, one can use the analytic Laplace solution of the radial pressure equation [*de Marsily*, 1986, p. 162]

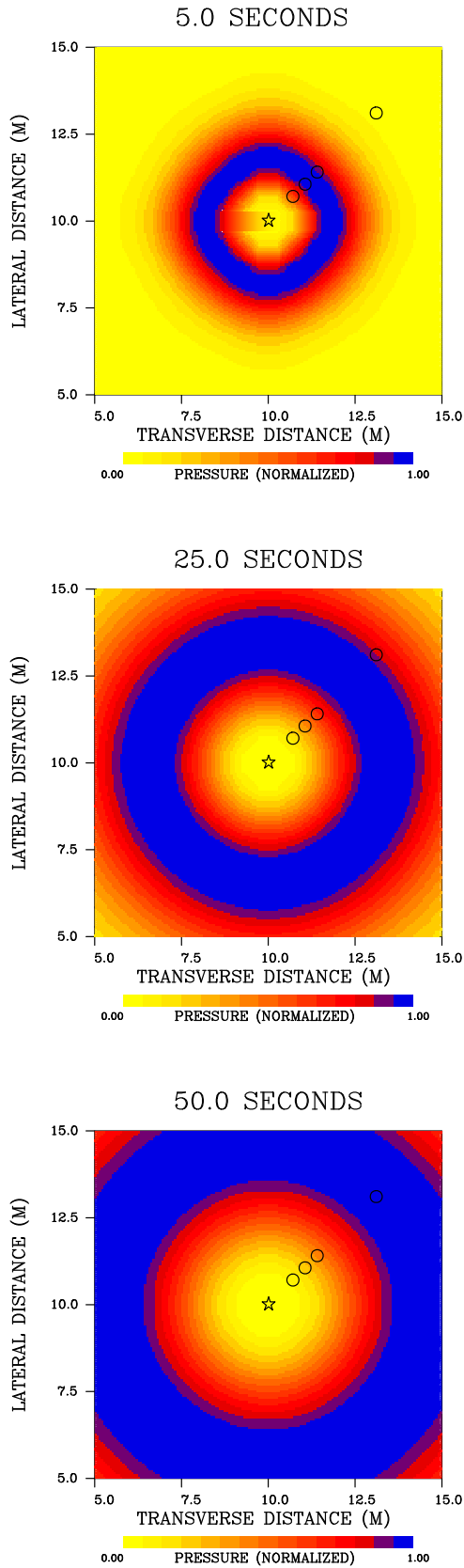$$P(r,t) = \frac{1}{t^{n/2}} \exp\left(-\frac{r^2}{4\Omega_h t}\right),\qquad(76)$$

where r is the radial distance from the source, Ω_h is

$$\Omega_h = \left(\frac{k}{\mu}\right)^{-1} \frac{1}{M},\qquad(77)$$

and n is the dimension of the medium, varying from 1 to 3. From expression (76) one can follow the procedure taken above and compute an analytic arrival time estimate. In Figure 6 both the asymptotic and the analytic arrival time estimates are shown, defined over the simulation grid. The asymptotic and analytic estimates are quite similar and generally agree with the numeric estimates plotted in Figure 5. In Figure 7 I have plotted the estimates along a line extending from the farthest well (well 4) to the injection well (central star in Figures 5 and 6) for a more detailed comparison. Note that there are differences between the numerical simulation and both the analytic and the asymptotic estimates. This is likely due to factors such as numerical dispersion, discretization effects, boundary effects, and induced anisotropy due to the grid orientation. For example, anisotropic propagation close to the source is evident when comparing the numerical travel times in Figure 5 to the analytic and asymptotic travel times in Figure 6.

3.2. Pressure Sensitive Permeability

[36] Having examined propagation in a poroelastic medium as a reference case, I now consider the situation in which the permeability is a function of the fluid pressure.

Figure 2.   Transient pressure variations associated with the four observation points on the simulation grid plotted in Figure 1. The pressure is indicated in meters of head. Well 1 is the well in Figure 1 that is closest to the injection point while well 4 is the farthest.

Figure 4. The normalized pressure variations over the central portion of the simulation grid. As in Figure 3, the time series at each grid point had been normalized by its peak value.
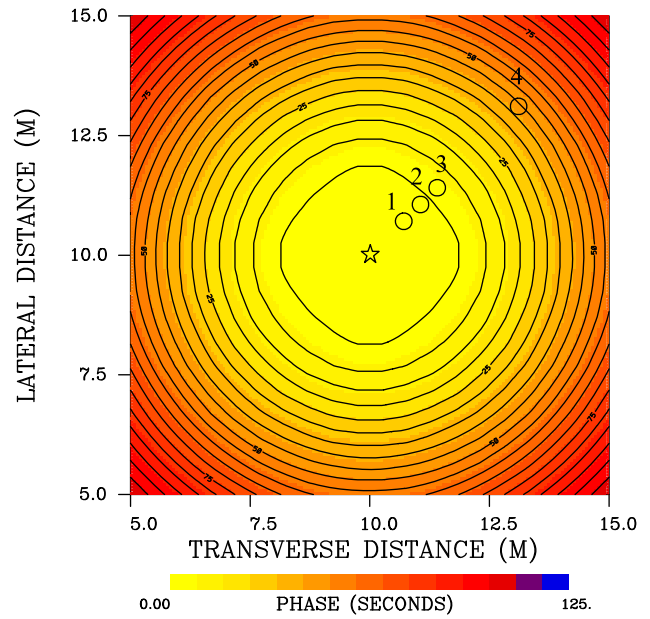
Figure 5. The arrival times associated with the numerical simulation. The time is estimated by finding the peak pressure value at each grid point and noting the time at which the peak was attained. The color scale indicates the travel time, as do the contours. The contour interval is 5 s.

The general conditions of the simulation are identical to those used to model the poroelastic propagation (Figure 1). That is, fluid is injected into a central source in a two dimensional layer. Four observation points are situated along a line extending from the source to the top right-hand corner of the simulation grid. Fluid is injected as an impulse, similar to a delta function. The coupled deformation and pressure changes are governed by the full set of equations (11) and (12).

[37] Unlike the poroelastic case, in which the medium properties did not change, here I will allow for properties that are functions of the fluid pressure. In particular, the permeability is assumed to be a linear function of the fluid pressure. In Figure 8 I plot the hydraulic conductivity, $K = k\rho g/\mu$, as a function of the fluid pressure. The pressure, indicated as meters of hydraulic head, varying from 0 to 150 m while the hydraulic conductivity varies by over an order of magnitude from 1.0×10^{-6} m s^{-1} to 3.8×10^{-5} m s^{-1}.

[38] The propagation of a coupled disturbance is governed by the partial differential equation for θ, equation (54). In what follows, the layer is assumed to be horizontal and gravitational effects are assumed to be negligible. Thus, equation (54) reduces to a nonlinear, first-order, scalar partial differential equation for θ,

$$\nabla\theta \cdot \nabla\theta - \Omega_v \frac{\partial\theta}{\partial t} = 0, \tag{78}$$

where

$$\Omega_v = \left(\beta_p \bar{P} + \frac{k}{\mu}\right)^{-1}\left[\alpha_p + \frac{\alpha\chi_p}{\frac{4}{3} - \chi_u}\right]. \tag{79}$$

Asymptotic
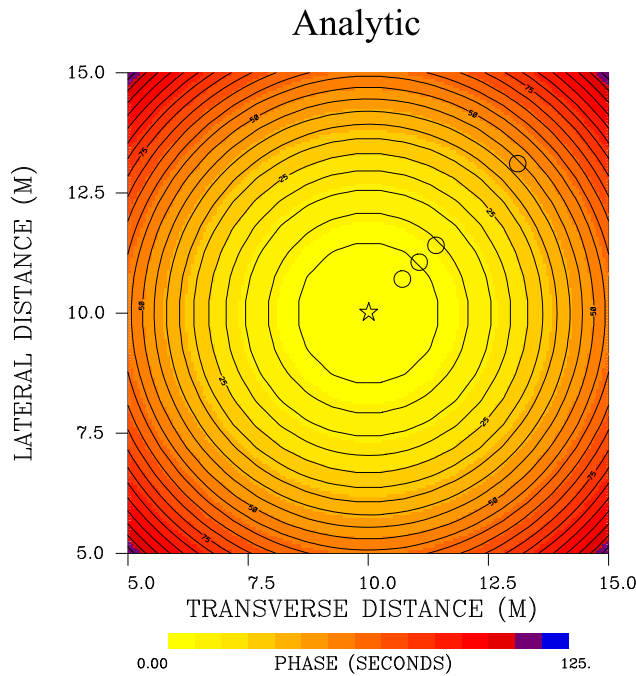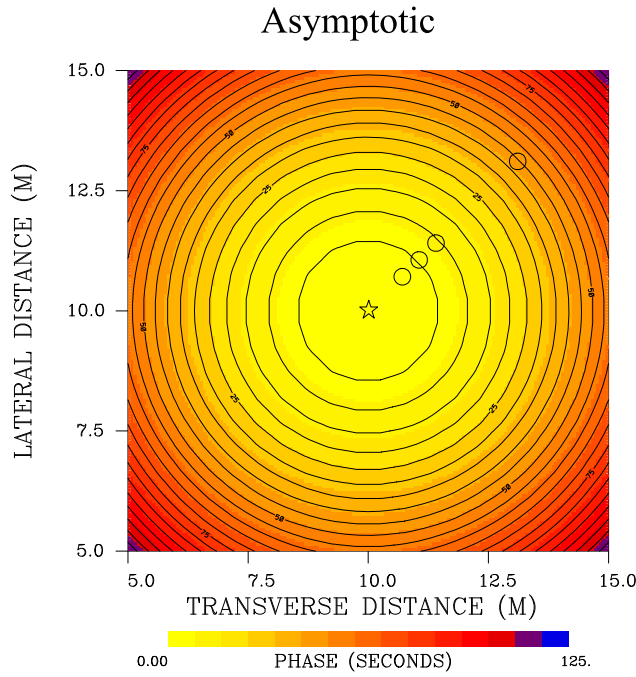
Analytic

Figure 6. (top) The asymptotic arrival time estimates associated with the simulation. (bottom) The arrival time estimates calculated using the analytic transient pressure solution for a porous medium (equation (76)).

Note that the propagation kinematics depend upon the quantity Ω_v and that, as indicated in (79), Ω_v depends upon the amplitude of the pressure change, through $\bar{P}$ (see equation (32)). Because of this dependence, one must rely upon a method, such as numerical simulation, in order to determine θ from equation (78).

[39] The importance of the expression (79) is that it indicates how Ω_v, the quantity that defines the differential
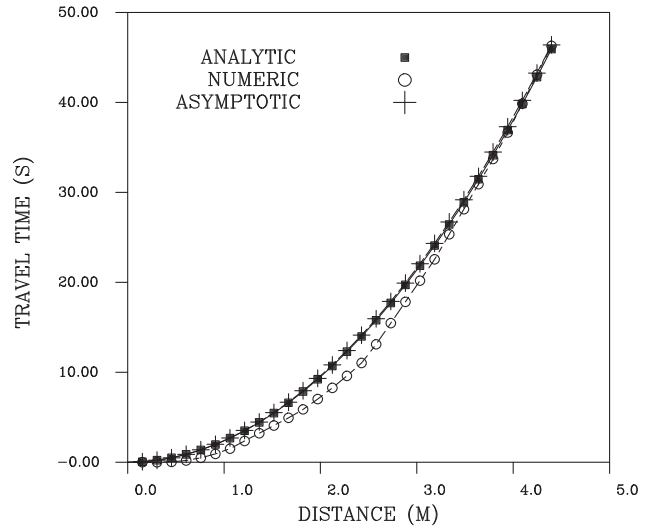

Figure 7. Travel time estimates for points on a northeast trending line extending from the central injection well to the farthest observation point. The numeric, the analytic, and the asymptotic estimates are shown.

equation (78) and hence determines θ, changes when the permeability becomes pressure dependent. The change due to the pressure dependence is simply that addition of the term $\beta_p \bar{P}$, where β_p is given by the expression (19), to the factor k/μ. Thus, the change in θ will only be significant in regions where $\bar{P}$ is sufficiently large relative to $k/\mu\beta_p$.

[40] As for the poroelastic medium, I have used TOCH-NOG [*Roddeman*, 2001] to simulate pressure and displacements for a medium in which the permeability, or the hydraulic conductivity, is a function of the fluid pressure, as indicated in Figure 8. The slope of the pressure–hydraulic
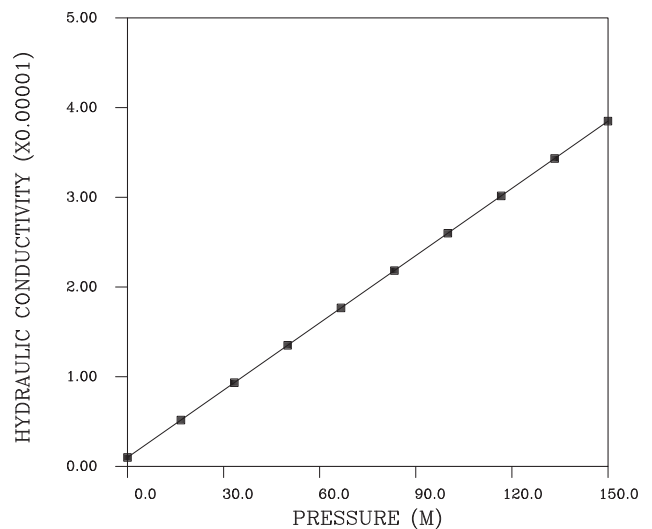

Figure 8. Pressure-permeability function used in the numerical simulation of transient pressure propagation. The fluid pressure is measured in meters of hydraulic head. The permeability k has been converted to hydraulic conductivity K, where $K = k\rho g/\mu$ for a fluid with density ρ and viscosity μ. The hydraulic conductivity is plotted in units of m s^{-1}.
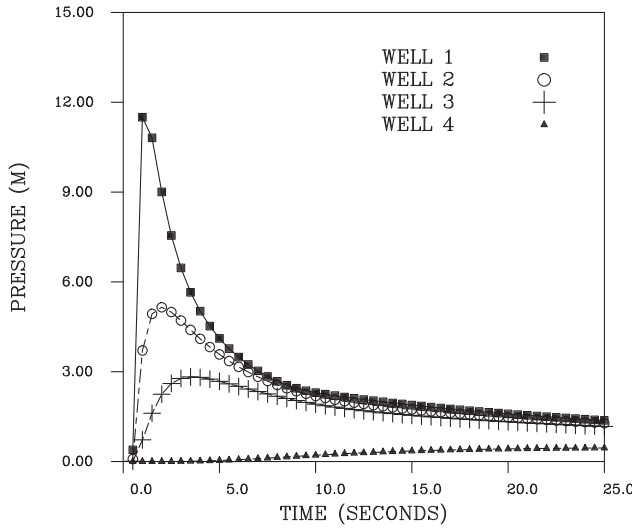
Figure 9. Transient pressure curves for the pressure-sensitive permeability simulation. The general simulation setup is identical to that shown in Figure 1, a central injector with four wells extending on a line to the northeast.

conductivity curve in this case is 2.5×10^{-7} s^{-1}. The routine TOCHNOG is capable of treating a medium in which the properties are arbitrary functions of pressure. The time-varying pressure at the four observation points, indicated by open circles in Figure 1, are shown in Figure 9. The general shape of the four curves are similar to those for the poroelastic medium (see Figure 2) The amplitude is significantly different however and the arrival times appear to have shifted. The arrival time shifts for the medium with pressure-dependent properties is clearer in the normalized plot (Figure 10), particularly for the three nearest observation points. This shift is clearly seen in Figure 11, a contour plot of the peak arrival times over the simulation grid. The innermost 5 s contour has shifted outward, indicating more rapid propagation closer to the injection well. Further from
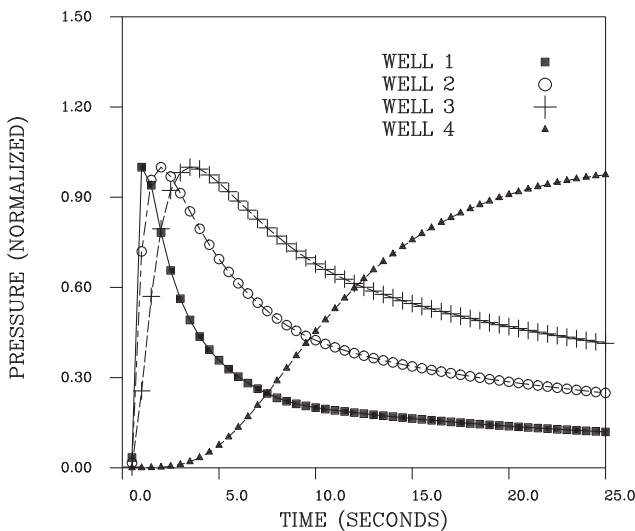
Figure 10. Normalized transient pressure curves for the four stations indicated in Figure 1.
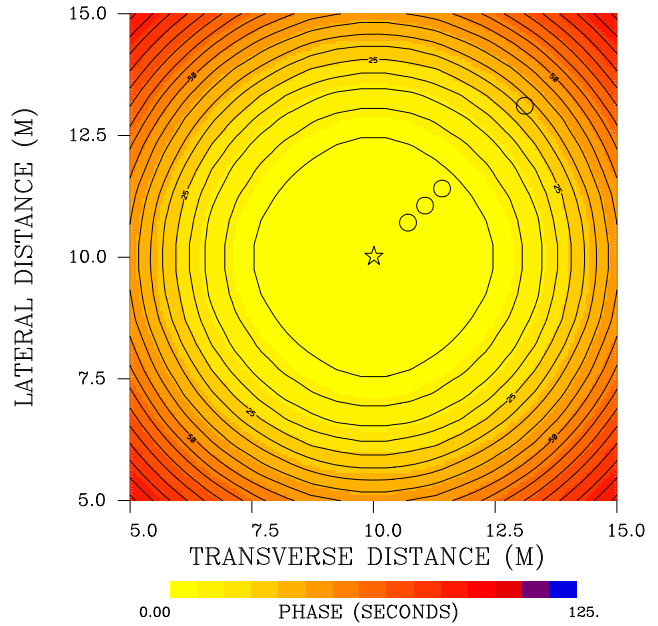
Figure 11. The arrival times associated with the numerical simulation. The color scale indicates the travel time, as do the contours. The contour interval is 5 s.

the injection well the spacing of the arrival time contours is similar to that of the poroelastic case (Figure 5).

[41] One could solve the scalar differential equation (78) in a straightforward fashion using a generalization of a finite difference approach [*Crandall and Lions*, 1983; *Crandall et al.*, 1984; *Vidale*, 1988; *Sethian*, 1990; *LeVeque*, 1992; *Lecomte*, 1993; *Sethian*, 1999; *Soukina et al.*, 2003]. The generalization involves including time as a variable in the velocity function Ω_v. This is easily accomplished by enlarging the dimension of the problem from three spatial dimensions to one involving four space-time dimensions. One can introduce a new variable representing the position along the trajectory in space time.

[42] The governing equation for $\theta(\mathbf{x}, t)$, equation (78), can also be solve using the method of characteristics noted above. Following the treatment of *Courant and Hilbert* [1962, p. 106], I write equation (78) in the form

$$\frac{\partial \theta}{\partial t} + F(\mathbf{x}, t, \mathbf{p}) = 0, \qquad (80)$$

where

$$F(\mathbf{x}, t, \mathbf{p}) = -\Omega_v^{-1} p^2 \qquad (81)$$

and $\Omega_v(\mathbf{x}, t)$, given by the expression (79), is a function of $\mathbf{x}$ and t that is assumed to be known. Here, I construct Ω_v using the properties of the medium and the pressure variation from the numerical simulation. As shown by the method of characteristics, the nonlinear, scalar, partial differential equation (80) is equivalent to the following system of ordinary equations

$$\frac{dx_i}{dt} = \frac{\partial F}{\partial p_i}, \qquad (82)$$

$$\frac{dp_i}{dt} = -\frac{\partial F}{\partial x_i}, \tag{83}$$

$$\frac{d\theta}{dt} = p^2 - F, \tag{84}$$

$$\frac{dp_t}{dt} = -\frac{\partial F}{\partial t}, \tag{85}$$

where $p_t = \partial\theta/\partial t$ and $i = 1, 2, 3$ [*Courant and Hilbert*, 1962, p. 106]. Equations (82)–(85) represent a system of eight equations in eight unknowns $[\mathbf{x}, \mathbf{p}, \theta, p_t]$. The system of equations define trajectories $\mathbf{x}(t)$ along which the solution $\theta(\mathbf{x}(t), t)$ are defined. The trajectories represent the path along which a disturbance propagates in the pressure-dependent medium. The geometry of the trajectories and the variation of the function $\theta(\mathbf{x}, t)$ depend upon the quantity $\Omega_v(\mathbf{x}, t)$, defined in the equation (79).

[43] The system of ordinary differential equations (82)–(85) may be solved numerically [*Press et al.*, 1992]. These equations are akin to the ray equations in electromagnetics [*Kline and Kay*, 1965; *Luneburg*, 1966; *Virieux et al.*, 1994] and elastic wave propagation [*Karal and Keller*, 1959; *Cerveny*, 1972; *Aki and Richards*, 1980; *Chapman*, 2004]. Ray methods have also been used in the study of various aspects of fluid flow. In particular, trajectory-based methods have been used in investigations of compressible fluid flow [*Shen*, 1983], transient pressure propagation [*Cohen and Lewis*, 1967; *Vasco et al.*, 2000], nonisothermal fluid flow [*Vasco*, 2010], and multiphase flow [*Vasco*, 2011]. Furthermore, a hybrid scheme has been developed in which numerical simulation is used to find the function θ and to used a set of reduced ray equations to find the solution trajectories [*Vasco and Finsterle*, 2004].

[44] Here I use a numerical technique to solve the ray equations. Note that the function Ω_v is a critical factor in defining the ray equations. Thus, the solution will depend strongly upon the function Ω_v. Furthermore, the pressure-dependent function Ω_v in equation (79) differs from the corresponding function for a porous medium, given by equation (59), because of the factor $\beta_p \bar{P}$. Thus, the function θ in a pressure-dependent medium should differ most strongly from that of an elastic porous medium in those regions where $\bar{P}$ is large in comparison to $k/(\mu\beta_p)$. In Figure 12 I plot the maximum amplitude obtained at each point of the simulation grid. The region of significant pressure change in near the injection well and encompasses the three innermost observation points. In Figure 13 I plot the travel time computed from solving the ray equations. Comparing Figure 13 to the estimates for the poroelastic medium (Figure 6), it seems that the largest changes do occur near the injection well. The travel time computed using the asymptotic expression is generally consistent with numeric estimate shown in Figure 11.

[45] In Figure 14 I provide a more detailed comparison for travel time estimates along a line extending from the injection well to the farthest observation well. There two sets of estimates generally agree. However, as in the poroelastic case (Figure 7) there are differences between the asymptotic and the numeric travel time estimates. These differences may be due to such factors as grid orientation,
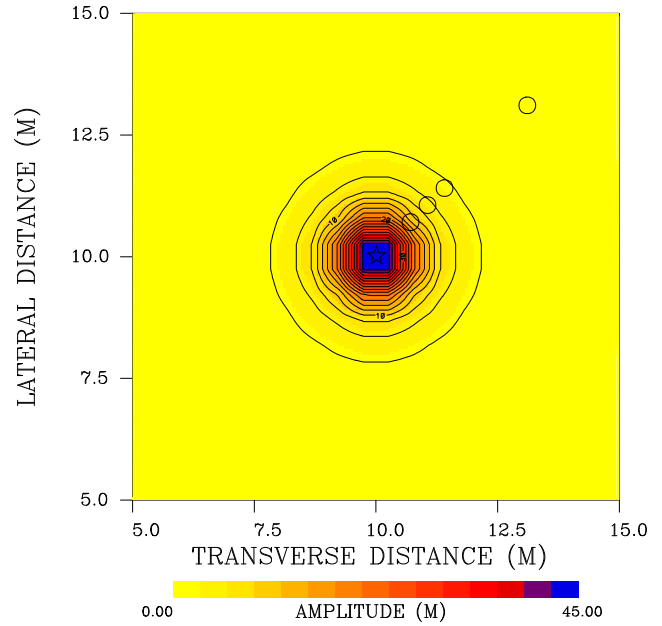
Figure 12. Peak pressure amplitude obtained at each point on the central portion of the simulation grid.

discretization, and dispersion effects. For example, there seems to be a slight asymmetry in the numeric travel time estimates shown in Figure 11. In addition, there may be some boundary effects, but these should be small for observation points close to the injection point.

[46] In order to examine the influence of the pressure dependence upon the travel times I varied the slope of the pressure curve. As noted above, the slope of the pressure-permeability curve in Figure 8 is 2.5×10^{-7} s^{-1}. For comparison, I tried slopes of 1.0×10^{-12} s^{-1}, 5.0×10^{-7} s^{-1},
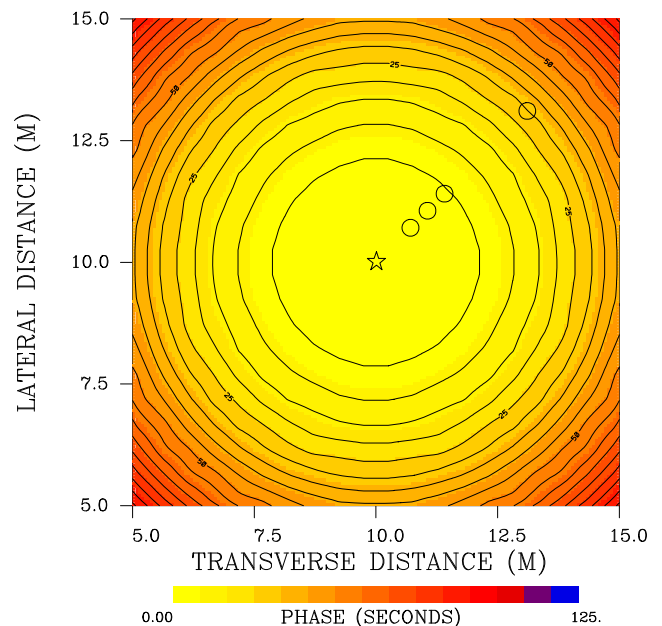
Figure 13. The arrival times associated with the asymptotic estimate. The color scale indicates the travel time, as do the contours. The contour interval is 5 s.
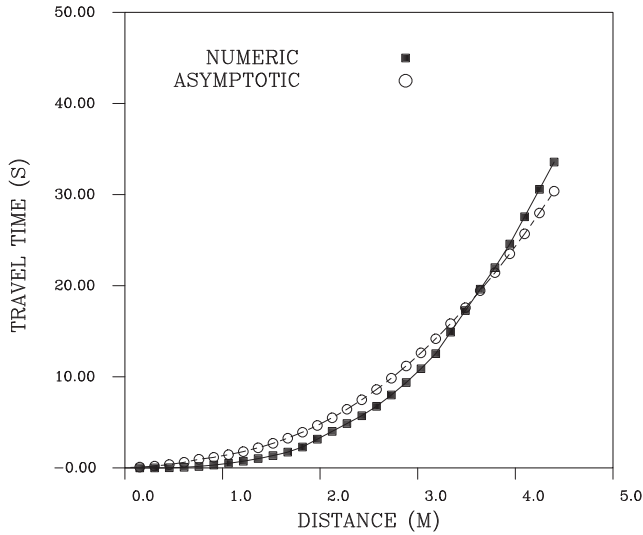
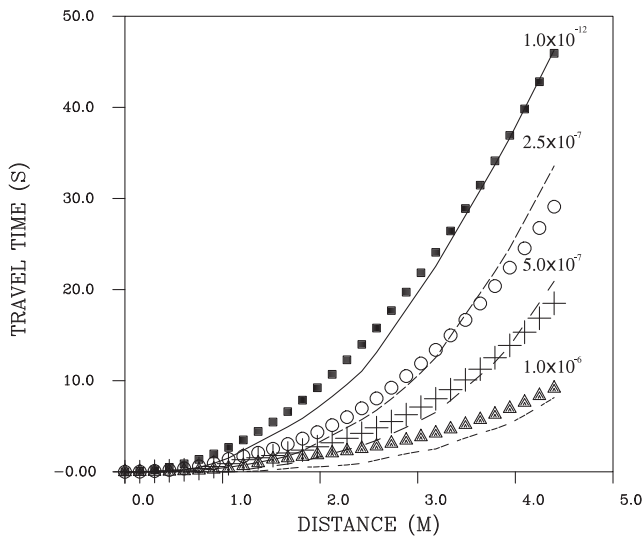**Figure 14.** Travel time estimates for points on a northeast trending line extending from the central injection well to the farthest observation point. The numeric and the asymptotic estimates are shown.

and 1.0×10^{-6} s^{-1}. The resulting travel time curves are shown in Figure 15. The travel times vary by almost an order of magnitude for the most distant points on the line, at about 4.5 km from the injection well. In general, the agreement between the numeric and the asymptotic estimates is reasonable, less then the differences between the

Figure 15. Travel time estimates for points on a northeast trending line extending from the central injection well to the farthest observation point. Each curve corresponds to a particular slope of a pressure-permeability curve, similar to that shown in Figure 8. The slope of each pressure-permeability curve is indicated by the label with units of m s^{-1} per meter of head, resulting in units of 1 s^{-1}. The continuous lines indicate the numerical estimates while the discontinuous points indicate the asymptotic estimates.

changes due to the variation in the slope of the pressure-permeability curve.

4. Conclusions

[47] In this paper I consider the propagation of a coupled displacement and pressure disturbance in a medium with pressure-dependent properties. For a disturbance propagating in a medium with smoothly varying properties an asymptotic technique may be used to derive a semianalytic solution. In particular, one may produce a scalar, first-order, partial differential equation for θ, a variable that is similar to the phase of a propagating wave. The coefficients of this differential equation are determined by the properties of the medium, including the pressure sensitivities of the medium parameters. The phase-like variable θ is also a function of the displacement and pressure amplitude variations across the propagating front. By the method of characteristics, this scalar, nonlinear partial differential equation is equivalent to a system of ordinary differential equations, the characteristic equations that define trajectories along which a solution may be defined. These equations are akin to the ray equations of electromagnetic and elastic ray theory.

[48] When the pressure sensitivities are set to zero the scalar equation and the travel time estimate reduce to the expressions for a poroelastic medium, as presented by *Vasco* [2008, 2009]. For a poroelastic medium the partial differential equation may be solved by the separation of variables. Thus, analytic travel time estimates are available for a poroelastic medium. The asymptotic estimates agree quite closely with the analytic values. There is general agreement between the asymptotic and analytic travel times and the travel times calculated using the numerical simulator TOCHNOG [*Roddeman*, 2001]. The discrepancies between the numerical simulation results and the analytic and asymptotic estimates are most likely due to discretization error, grid orientation effects, and boundary effects.

[49] For a medium with pressure-dependent permeability the semianalytic coefficients of the scalar equation for θ indicate that the largest differences will occur where the pressure changes are greatest. Both the numerical simulation and the asymptotic estimates indicate that this is indeed the case, with the largest phase changes near the injection well where the pressure increase is the largest. As was the case for the poroelastic medium, there is general agreement between the numeric travel time estimates and the asymptotic estimates. A comparison for several pressure-permeability curves indicates overall agreement between the numerical simulation and the asymptotic travel times.

[50] This study could be extended in several respects. First, one could allow other parameters, such as the geomechanical properties, to be functions of pressure. Second, the parameters are typically sensitive to the effective pressure which involves the confining pressure as well as the fluid pressure [*Terzaghi*, 1943; *Jaeger et al.*, 2007]. Third, it is possible to consider the full set of governing equations, including the inertial terms that give rise to the fast modes of propagation. Such terms were considered for a poroelastic medium in the study of *Vasco* [2009]. Also, one could allow for both pressure- and deformation-dependent properties. Finally, there are more general models of solid deformation, including plastic deformation that may be used

[*Ehlers*, 1992; *Bertram*, 2008] in place of the nonlinear elastic model adopted here. The asymptotic approach used in this paper is general and can be applied to these and other problems.

Appendix A: Constitutive Relationships

[51] In this appendix I derive constitutive relationships associated with a deformable porous medium saturated with a single viscous fluid. The hypothetical medium will represent a consolidated material, such as a cemented sandstone, a limestone, or an intact metamorphic or igneous material. Thus, while there may be fractures or microfractures, the component particles are cemented. The change in fluid pressure and effective stress may be large over the time interval of interest, but not so large as to induce plastic deformation or the crushing of individual grains. Thus, the constituent particles remain intact and do not rotate nor do they migrate with respect to one another. However, because of processes such as changing grain contact area and fracture opening or closing with pressure or stress changes, the rock as a whole may deform in a nonlinear fashion. That is, the stress may not vary linearly with the strain. For example, it is well known that the variation in contact area for compressed grains as a function of pressure leads to pressure-dependent elastic moduli and wave speeds [*Mindlin*, 1949; *Johnson*, 1985; *Goddard*, 1990; *Zimmerman*, 1991; *Makse et al.*, 2004]. Because the processes of grain contact area changes and fracture opening and closing are reversible, the rock returns to its original configuration upon the release of the fluid pressure or stress changes. Thus, the body does behave as an elastic solid, albeit as a nonlinear elastic solid. The similarities and differences between such a model and a simple elastic-plastic model were given by *Nelson and Baron* [1971].

[52] The many formulations of nonlinear elastic solids precludes a complete listing. One can consult the numerous texts treating nonlinear elastic behavior [*Murnaghan*, 1951; *Eringen*, 1962; *Goldenblat*, 1962; *Brillouin*, 1964; *Truesdell and Noll*, 1965; *Jaunzemis*, 1967; *Ogden*, 1984; *Bertram*, 2008]. Treatments of a nonlinear poroelastic solid containing a fluid are much more limited, perhaps because of the complexity of the topic. Nonetheless, there are a number of studies [*Biot and Willis*, 1957; *Morland*, 1972; *Biot*, 1973; *Lewis and Schrefler*, 1978; *Ehlers*, 1992; *de Boer*, 2000, p. 377; *Bemer et al.*, 2001; *Cheng and Abousleiman*, 2008] from which to draw upon when treating a nonlinear poroelastic medium.

A1. Physical Properties of the Porous Medium

[53] In what follows I shall generalize an approach based upon strain invariants, as presented by *Goldenblat* [1962]. As in the works by *Biot* [1973] and *Bemer et al.* [2001], I include variables for fluid pressure and volumetric fluid content. As a starting point, consider a fluid-filled porous medium with fairly general relationships between the solid stress tensor σ, solid strain ϵ, the fluid pressure P_f, and the change in volumetric fluid content ς

$$\sigma_{ij} = S_{ij}(\boldsymbol{\epsilon}, P_f) \tag{A1}$$

$$\varsigma = F(\boldsymbol{\epsilon}, P_f). \tag{A2}$$

Equations of the form (A1) and (A2) are appropriate for a very general medium. I shall invoke several approximations in order to treat a specific behavior. In particular, I shall assume that the medium has isotropic properties, that the deformation is small, and the medium behaves as a nonlinear elastic body.

[54] For an isotropic medium the physical laws describing the deformation must be independent of the coordinate system used to represent the problem. Thus, one may express the relationship in terms of quantities that are independent of the particular system of coordinates. Thus, I can write the equations (A1) and (A2) in terms of the invariants of the tensor ϵ. Note that a scalar, such as P_f, is already invariant with respect to coordinate transformations. While, for any given tensor, there are an infinite number of invariants [*Goldenblat*, 1962], a theorem first proved by Hilbert [*Cox et al.*, 1998] demonstrates that all invariants may be generated by a finite collection of fundamental, or basis, invariants. For example, in the case of the strain tensor ϵ, a 3 by 3 array, there are three fundamental invariants I_1, I_2, and I_3, given by [*Goldenblat*, 1962, p. 7]

$$I_1 = \delta_{ik}\epsilon_{ik} = \epsilon_{ii} = \epsilon_{11} + \epsilon_{22} + \epsilon_{33}, \tag{A3}$$

$$I_2 = \epsilon_{ik}\epsilon_{ik}, \tag{A4}$$

$$I_3 = \epsilon_{ik}\epsilon_{kp}\epsilon_{pi}, \tag{A5}$$

where, as indicated in equation (A3), I have invoked the Einstein convention by which one sums over repeated indices. Note that these three invariants are related to the coefficient of the cubic equation that determines the eigenvalues of the ϵ [*Murnaghan*, 1951, p. 36; *Ogden*, 1984, p. 25]. Also, note that while the invariant (A3) is the trace of the matrix ϵ, the invariant I_2 is a measure of the norm of ϵ, the sum of the squares of the components of the strain matrix.

[55] One may expand the functions S_{ij} and F as power series in the components of the strain tensor ϵ and the fluid pressure P_f

$$\begin{aligned} S_{ij}(\epsilon, P_f) = {} & S_0\delta_{ij} + S_\epsilon\epsilon_{ij} + S_pP_f\delta_{ij} + S_{\epsilon\epsilon}\epsilon_{ik}\epsilon_{kj} \\ & + S_{p\epsilon}P_f\epsilon_{kj}\delta_{ik} + S_{p\epsilon}P_f{}^2\delta_{ij} + \cdots \end{aligned} \tag{A6}$$

$$\begin{aligned} F(\boldsymbol{\epsilon}, P_f) = {} & F_0 + F_\epsilon\epsilon_{ij}\delta_{ij} + F_pP_f \\ & + F_{\epsilon\epsilon}\epsilon_{ik}\epsilon_{kj}\delta_{ij} + F_{p\epsilon}P_f\epsilon_{ij}\delta_{ij} + F_{p\epsilon}P_f{}^2 + \cdots. \end{aligned} \tag{A7}$$

As indicated by *Goldenblat* [1962, p. 7], one may write the power series in terms of the tensor invariants and, as noted above, the invariants may be generated by the three basis functions I_1, I_2, and I_3. Thus, the above series representations may be written, without approximation, as

$$\begin{aligned} \sigma_{ij} = {} & T_0(I_1, I_2, I_3, P_f)\delta_{ij} + T_1(I_1, I_2, I_3, P_f)\epsilon_{ij} \\ & + T_2(I_1, I_2, I_3, P_f)\epsilon_{ik}\epsilon_{kj} \end{aligned} \tag{A8}$$

$$\begin{aligned} \varsigma = {} & V_0(I_1, I_2, I_3, P_f) + V_1(I_1, I_2, I_3, P_f)\epsilon_{ij}\delta_{ij} \\ & + V_2(I_1, I_2, I_3, P_f)\epsilon_{ik}\epsilon_{kj}\delta_{ij}. \end{aligned} \tag{A9}$$

Using the invariants minimizes the number of parameters required to relate the stresses and fluid volume to the strains and the fluid pressure. For deformation involving small strains, equations (A8) and (A9) may be reduced further by neglecting the highest-order terms, giving

$$\sigma_{ij} = T_0(I_1, I_2, P_f)\delta_{ij} + T_1(I_1, I_2, P_f)\epsilon_{ij} \quad \text{(A10)}$$

$$\varsigma = V_0(I_1, I_2, P_f) + V_1(I_1, I_2, P_f)\epsilon_{ij}\delta_{ij}. \quad \text{(A11)}$$

Note that the stress-strain relationship given above may be nonlinear because of the functional coefficients T_0, T_1, V_0, and V_1. However, the stress and the change in fluid volume do return to their background values if the strain and any changes in fluid pressure vanish.

[56] Equations (A8) and (A9) can be related to expressions derived in previous studies of nonlinear elastic porous media. For example, *Biot*'s [1973] study of a semilinear porous solid and a follow-up study by *Bemer et al.* [2001] produced the expressions

$$\sigma_{ij} = (\lambda I_1 - \alpha P_f)\delta_{ij} + 2G\epsilon_{ij} + \frac{\partial H}{\partial \epsilon_{ij}} \quad \text{(A12)}$$

$$\varsigma = \alpha I_1 + \frac{1}{M}P_f - \frac{\partial H}{\partial \epsilon_{ij}}\delta_{ij}, \quad \text{(A13)}$$

where λ is a Lame constant, α is a coupling constant, G is the shear modulus, and H is a function of the three invariants I_1, I_2, and I_3,

$$H(I_1, I_2, I_3) = \frac{D}{3}I_1^3 + (F - D)(I_1 I_2 - 3I_3), \quad \text{(A14)}$$

and the coefficients D and F characterize the nonlinear behavior of the porous solid. This approach of *Biot* [1973] and *Bemer et al.* [2001] was formulated for a semilinear solid in which the solid constituents of the porous medium deform linearly while the material as a whole may deform nonlinearly. The idea is that the solid grains behave in a linear elastic manner, but the rock as a whole, containing microcracks and interacting grains, behaves elastically but not linearly. A similar representation of the constitutive laws for a fluid saturated porous rock in terms of invariants was presented by *Morland* [1972], although the approach was based upon mixture theory.

[57] The stress-strain and fluid volume–strain relationships (A10) and (A11) can also be used to represent strain- and pressure-dependent moduli. Such moduli are useful for modeling the behavior of soils, granular material, and fractured material [*Nelson and Baron*, 1971]. For example, one may have define a bulk modulus that depends upon the trace of the strain tensor, related to the mean strain, via

$$K = K_0 + K_1 I_1 + K_2 I_1^2 \quad \text{(A15)}$$

or a bulk modulus that depends upon the effective pressure P [*Nelson and Baron*, 1971],

$$K = K_0 + K_1 P + K_2 P^2. \quad \text{(A16)}$$

In this paper I will primarily be interested in the injection of fluid, possibly at high pressures, into a porous medium. I shall assume that the pressure changes are sufficient to change the characteristics of the porous material, particularly the flow properties. Furthermore, I assume that the overburden stress on the material is primarily due to the weight of the overlying material and thus does not change significantly. Also, the strain within the porous material is taken to be so small that it does not significantly alter the mechanical or flow properties of the rock. Thus, I begin with the expressions (A10) and (A11) of the form

$$\sigma_{ij} = T_0(I_1, P_f)\delta_{ij} + T_1(P_f)\epsilon_{ij} \quad \text{(A17)}$$

$$\varsigma = V_0(P_f) + V_1(P_f)I_1, \quad \text{(A18)}$$

where I have used the fact that $I_1 = \epsilon_{ii} = \epsilon_{ij}\delta_{ij}$. The strains are assumed to be small enough so that product terms may be neglected and the strain tensor may be represented by the infinitesimal strain tensor [*Eringen*, 1962, p. 16]

$$\boldsymbol{\epsilon} = \frac{1}{2}(\nabla\mathbf{u} + \nabla\mathbf{u}^T). \quad \text{(A19)}$$

The invariant I_1, the trace of the strain tensor $\boldsymbol{\epsilon}$, is given by

$$I_1 = \epsilon_{11} + \epsilon_{22} + \epsilon_{33} = \text{tr}(\boldsymbol{\epsilon}) = \nabla \cdot \mathbf{u}, \quad \text{(A20)}$$

so that I can write equations (A17) and (A18) as

$$\sigma_{ij} = T_0(\nabla \cdot \mathbf{u}, P_f)\delta_{ij} + T_1(P_f)\epsilon_{ij} \quad \text{(A21)}$$

$$\varsigma = V_0(P_f) + V_1(P_f)\nabla \cdot \mathbf{u}. \quad \text{(A22)}$$

In order to express equations (A21) and (A22) in a manner compatible with the work of *Biot* [1973] and *Bemer et al.* [2001] and so that they will agree with the expressions for linear poroelastic media, I write them as

$$\sigma_{ij} = G\left(2\epsilon_{ij} - \frac{2}{3}\nabla \cdot \mathbf{u}\delta_{ij}\right) - \varphi_u \nabla \cdot \mathbf{u}\delta_{ij} - \alpha_m P_f\delta_{ij} \quad \text{(A23)}$$

$$\varsigma = \varphi_m P_f + \alpha_m \nabla \cdot \mathbf{u}. \quad \text{(A24)}$$

Defining the tensor

$$\Sigma = \nabla\mathbf{u} + \nabla\mathbf{u}^T - \frac{2}{3}\nabla \cdot \mathbf{u}\mathbf{I} \quad \text{(A25)}$$

and making use of equation (A19), I can write equations (A23) and (A24) in the form

$$\boldsymbol{\sigma} = G\Sigma - \varphi_u \nabla \cdot \mathbf{u}\mathbf{I} - \alpha_m P_f\mathbf{I} \quad \text{(A26)}$$

$$\nabla \cdot \mathbf{w} = -\varphi_m P_f - \alpha_m \nabla \cdot \mathbf{u}, \quad \text{(A27)}$$

where I have made use of the fact that the increment of fluid content may be written as

$$\varsigma = -\nabla \cdot \mathbf{w} \quad \text{(A28)}$$

[*Biot*, 1941; *Wang*, 2000], where **w** is the fluid displacement relative to the displacement of the solid matrix:

$$\mathbf{w} = \phi(\mathbf{u}_f - \mathbf{u}), \tag{A29}$$

where $\mathbf{u}_f$ is the fluid displacement vector and ϕ is the porosity [*Pride*, 2005]. Note that the coefficients in equations (A26) and (A27), G, φ_u, α_u, φ_m and α_m may be functions of the fluid pressure P_f and functions of spatial position.

[58] Using the expression

$$P_f = -C\nabla \cdot \mathbf{u} - M\nabla \cdot \mathbf{w} \tag{A30}$$

from *Pride* [2005], I can relate the coefficients φ_m and α_m to *Biot*'s [1962] C modulus and the fluid storage coefficient M which represents how much fluid can accumulate when the fluid pressure changes at a constant sample size. Solving equation (A30) for $\nabla \cdot \mathbf{w}$ gives

$$\nabla \cdot \mathbf{w} = -\frac{1}{M}P_f - \frac{C}{M}\nabla \cdot \mathbf{u}, \tag{A31}$$

and so

$$\varphi_m = \frac{1}{M} \tag{A32}$$

$$\alpha_m = \frac{C}{M}. \tag{A33}$$

Another expression from *Pride* [2005] gives the stress tensor as

$$\boldsymbol{\sigma} = G\Sigma + K_u\nabla \cdot \mathbf{u}\mathbf{I} + C\nabla \cdot \mathbf{w}\mathbf{I}. \tag{A34}$$

Using equation (A30) this expression may be written in terms of $\nabla \cdot \mathbf{u}$ and P_f:

$$\boldsymbol{\sigma} = G\Sigma + \left(K_u - \frac{C^2}{M}\right)\nabla \cdot \mathbf{u}\mathbf{I} - \frac{C}{M}P_f\mathbf{I}, \tag{A35}$$

given $\alpha_m = C/M$, as before, and

$$\varphi_u = \frac{C^2}{M} - K_u, \tag{A36}$$

where K_u is the undrained bulk modulus. Thus, the quantities given above may be interpreted in terms of existing poroelastic coefficients.

[59] In addition to the parameters associated with stress-strain, fluid mass, and pressure constitutive equations, there are also flow properties, such as the porosity ϕ and permeability k, associated with a porous medium. These properties are typically measured in the laboratory, when they are available, and fit in some empirical fashion. However, expressions may be obtained from conceptual models such as analytic fracture models [*Witherspoon et al.*, 1980].

A2. Fluid Properties

[60] Typically, the fluid properties are determined in the laboratory and are much better characterized then are the properties of the porous rock. For example, in the applications I shall consider a situation in which water injected into a pressure sensitive rock. Because of its importance in many processes, the physical properties of water are extremely well known and there is a generally accepted equation of state for the density as a function of pressure [*Bear* 1972, p. 38; *de Marsily*, 1986, p. 40]

$$\rho = \rho_0\exp\beta(P_f - P_0). $$

Other fluids and fluid mixtures can behave differently, for example supercritical carbon dioxide can act much like a gas. There are also accurate tabulations of the viscosity of water and other fluids as functions of temperature and pressure [*de Marsily*, 1986, p. 414].

Appendix B: An Asymptotic Analysis of the Governing Equations

[61] The governing equations (11) and (12) are rather formidable, with pressure-dependent and spatially varying coefficients, nonlinear terms, and coupled dependent variables. If one is to make progress and gain some insight, one must simplify the system of equations in some manner. As noted above, because I am interested in the inverse problem in which I estimate the large-scale variation of properties, one possible simplifying assumption is that the medium is smoothly varying. That is, away from boundaries, such as faults and layering, the material properties vary in a smooth fashion. Specifically, the length scale of the heterogeneity of the medium, denoted by L is much larger than the length scale, l, of the propagating disturbances that I am modeling. So I can define a scale parameter $\varepsilon = l/L \ll 1$ and define "slow" spatial and temporal coordinates

$$\mathbf{X} = \varepsilon\mathbf{x} \tag{B1}$$

$$T = \varepsilon t, \tag{B2}$$

respectively. The first step in such an analysis entails writing the governing equations (11) and (12) in the slow coordinate system. To do this I formulate the differential operators in terms of the new coordinates. Thus, the time derivative becomes

$$\frac{\partial P}{\partial t} = \varepsilon\frac{\partial P}{\partial T} + \frac{\partial \theta_p}{\partial t}\frac{\partial P}{\partial \theta_p}. \tag{B3}$$

The differential operators in the governing equations may be written in terms of the slow variable $\mathbf{X}$ by noting that

$$\frac{\partial \mathbf{u}}{\partial x_i} = \varepsilon\frac{\partial \mathbf{u}}{\partial X_i} + \frac{\partial \theta}{\partial x_i}\frac{\partial \mathbf{u}}{\partial \theta}. \tag{B4}$$

Hence, making use of equation (B1) I can write the gradient operators as

$$\nabla\mathbf{u} = \varepsilon\nabla_X\mathbf{u} + \nabla\theta\frac{\partial \mathbf{u}}{\partial \theta} \tag{B5}$$

$$\nabla \cdot \mathbf{u} = \varepsilon \nabla_X \cdot \mathbf{u} + \nabla \theta \cdot \frac{\partial \mathbf{u}}{\partial \theta}, \tag{B6}$$

where ∇_X denotes the gradient with respect to the components of the slow variable $\mathbf{X}$. In the derivation that follows I shall suppress the X subscript on the differential operator ∇.

B1. Analysis of the First Governing Equation

[62] I begin with the first of the two governing equations, equation (11)

$$\nabla \cdot \Sigma + \nabla \zeta \cdot \Sigma + \gamma_p \nabla P \cdot \Sigma - \eta \nabla \varphi_u \nabla \cdot \mathbf{u}$$
$$- \kappa_u \nabla P \nabla \cdot \mathbf{u} - \chi_u \nabla \nabla \cdot \mathbf{u} - \eta \nabla \alpha P - \chi_p \nabla P = 0. \tag{B7}$$

Writing equation (B7) in slow coordinates, transforming the derivatives,

$$\left(\varepsilon \nabla \cdot \Sigma + \nabla \theta_u \cdot \frac{\partial \Sigma}{\partial \theta_u} \right) + \varepsilon \nabla \zeta \cdot \Sigma + \gamma_p \left(\varepsilon \nabla P + \nabla \theta_p \frac{\partial P}{\partial \theta_p} \right) \cdot \Sigma$$
$$- \varepsilon \nabla \varphi_u \left(\varepsilon \nabla \cdot \mathbf{u} + \nabla \theta_u \cdot \frac{\partial \mathbf{u}}{\partial \theta_u} \right) - \kappa_u \left(\varepsilon \nabla P + \nabla \theta_p \frac{\partial P}{\partial \theta_p} \right)$$
$$\cdot \left(\varepsilon \nabla \cdot \mathbf{u} + \nabla \theta_u \cdot \frac{\partial \mathbf{u}}{\partial \theta_u} \right) - \chi_u \left[\varepsilon \nabla \left(\varepsilon \nabla \cdot \mathbf{u} + \nabla \theta_u \cdot \frac{\partial \mathbf{u}}{\partial \theta_u} \right) \right.$$
$$\left. - \nabla \theta_u \frac{\partial}{\partial \theta_u} \left(\varepsilon \nabla \cdot \mathbf{u} + \nabla \theta_u \cdot \frac{\partial \mathbf{u}}{\partial \theta_u} \right) \right] - \epsilon \eta \nabla \alpha P$$
$$- \chi_p \left(\varepsilon \nabla P + \nabla \theta_p \frac{\partial P}{\partial \theta_p} \right) = 0. \tag{B8}$$

Because I am assuming that ε is small, all terms of order ε and higher are neglected, leaving terms of order $\varepsilon^0 \sim 1$:

$$\nabla \theta_u \cdot \frac{\partial \Sigma}{\partial \theta_u} + \gamma_p \nabla \theta_p \cdot \Sigma \frac{\partial P}{\partial \theta_p} - \kappa_u \nabla \theta_p \frac{\partial P}{\partial \theta_p} \nabla \theta_u \cdot \frac{\partial \mathbf{u}}{\partial \theta_u}$$
$$- \chi_u \nabla \theta_u \nabla \theta_u \cdot \frac{\partial^2 \mathbf{u}}{\partial \theta_u^2} - \chi_p \nabla \theta_p \frac{\partial P}{\partial \theta_p} = 0. \tag{B9}$$

Using the fact that $\Sigma = \nabla \mathbf{u} + \nabla \mathbf{u}^T - \frac{2}{3} \nabla \cdot \mathbf{u}\mathbf{I}$, writing the differential operators in slow coordinates, and neglecting terms of order greater than zero gives

$$\nabla \theta_u \cdot \left[\nabla \theta_u \frac{\partial^2 \mathbf{u}}{\partial \theta_u} + \frac{\partial^2 \mathbf{u}}{\partial \theta_u} \nabla \theta_u - \frac{2}{3} \mathbf{I} \nabla \theta_u \cdot \frac{\partial^2 \mathbf{u}}{\partial \theta_u} \right]$$
$$+ \gamma_p \frac{\partial P}{\partial \theta_p} \nabla \theta_p \cdot \left[\nabla \theta_u \frac{\partial \mathbf{u}}{\partial \theta_u} + \frac{\partial \mathbf{u}}{\partial \theta_u} \nabla \theta_u - \frac{2}{3} \mathbf{I} \nabla \theta_u \cdot \frac{\partial \mathbf{u}}{\partial \theta_u} \right]$$
$$- \kappa_u \nabla \theta_p \frac{\partial P}{\partial \theta_p} \nabla \theta_u \cdot \frac{\partial \mathbf{u}}{\partial \theta_u} - \chi_u \nabla \theta_u \nabla \theta_u \cdot \frac{\partial^2 \mathbf{u}}{\partial \theta_u^2} - \chi_p \nabla \theta_p \frac{\partial P}{\partial \theta_p} = 0. \tag{B10}$$

This expression can be written more compactly if one defines the phase gradient vectors

$$\mathbf{p} = \nabla \theta_p \tag{B11}$$

$$\mathbf{s} = \nabla \theta_u. \tag{B12}$$

Further more, because of the specific form chosen for the asymptotic expansion, equation (24) or (25), in particular the functional dependence of the solution on the phase terms θ_p and θ_u, the partial derivatives are given by

$$\frac{\partial P}{\partial \theta_p} = P - P_b = \bar{P} \tag{B13}$$

$$\frac{\partial \mathbf{u}}{\partial \theta_u} = \mathbf{u} - \mathbf{u}_b = \bar{\mathbf{U}}, \tag{B14}$$

and similarly for higher-order derivatives.

[63] Substituting these definitions into equation (B10) gives

$$\mathbf{s} \cdot \left[\mathbf{s}\bar{\mathbf{U}} + \bar{\mathbf{U}}\mathbf{s} - \frac{2}{3} \mathbf{Is} \cdot \bar{\mathbf{U}} \right] + \gamma_p \bar{P}\mathbf{p} \cdot \left[\mathbf{s}\bar{\mathbf{U}} + \bar{\mathbf{U}}\mathbf{s} - \frac{2}{3} \mathbf{Is} \cdot \bar{\mathbf{U}} \right] \tag{B15}$$
$$- \kappa_u \mathbf{p}\bar{P}\mathbf{s} \cdot \bar{\mathbf{U}} - \chi_u \mathbf{ss} \cdot \bar{\mathbf{U}} - \chi_p \mathbf{p}\bar{P} = 0,$$

or, carrying out the dot products,

$$\left[s^2 \bar{\mathbf{U}} + \frac{1}{3}(\mathbf{s} \cdot \bar{\mathbf{U}})\mathbf{s} \right] + \gamma_p \bar{P} \left[\mathbf{p} \cdot \mathbf{s}\bar{\mathbf{U}} + (\mathbf{p} \cdot \bar{\mathbf{U}})\mathbf{s} - \frac{2}{3}(\mathbf{s} \cdot \bar{\mathbf{U}})\mathbf{p} \right]$$
$$- \kappa_u \bar{P}(\mathbf{s} \cdot \bar{\mathbf{U}})\mathbf{p} - \chi_u (\mathbf{s} \cdot \bar{\mathbf{U}})\mathbf{s} - \chi_p \bar{P}\mathbf{p} = 0. \tag{B16}$$

B2. Analysis of the Second Governing Equation

[64] Now consider equation (12), the governing equation associated with the fluid diffusion,

$$\alpha_p \frac{\partial P}{\partial t} + \alpha_u (\nabla \cdot \mathbf{u}) \frac{\partial P}{\partial t} + \alpha \frac{\partial \nabla \cdot \mathbf{u}}{\partial t} - \frac{1}{\mu} \nabla k \cdot \nabla P$$
$$- \beta_p \nabla P \cdot \nabla P - \gamma \nabla P \cdot \mathbf{g} - \frac{1}{\mu} \nabla k \cdot \mathbf{g} - \frac{k}{\mu} \nabla \cdot \nabla P = 0. \tag{B17}$$

Writing this equation in slow coordinates, expanding the derivatives, gives

$$\alpha_p \left(\varepsilon \frac{\partial P}{\partial T} + \frac{\partial \theta_p}{\partial t} \frac{\partial P}{\partial \theta_p} \right) + \alpha_u \left(\varepsilon \nabla \cdot \mathbf{u} + \frac{\partial \mathbf{u}}{\partial \theta_u} \cdot \nabla \theta_u \right)$$
$$\cdot \left(\varepsilon \frac{\partial P}{\partial T} + \frac{\partial \theta_p}{\partial t} \frac{\partial P}{\partial \theta_p} \right) + \alpha \left[\varepsilon \frac{\partial}{\partial T} \left(\varepsilon \nabla \cdot \mathbf{u} + \frac{\partial \mathbf{u}}{\partial \theta_u} \cdot \nabla \theta_u \right) \right.$$
$$\left. + \frac{\partial \theta_u}{\partial t} \frac{\partial}{\partial \theta_u} \left(\varepsilon \nabla \cdot \mathbf{u} + \frac{\partial \mathbf{u}}{\partial \theta_u} \cdot \nabla \theta_u \right) \right] - \frac{1}{\mu} \varepsilon \nabla k$$
$$\cdot \left(\varepsilon \nabla P + \frac{\partial P}{\partial \theta_p} \nabla \theta_p \right) - \beta_p \left(\varepsilon \nabla P + \nabla \theta_p \frac{\partial P}{\partial \theta_p} \right)$$
$$\cdot \left(\varepsilon \nabla P + \nabla \theta_p \frac{\partial P}{\partial \theta_p} \right) - \gamma \left(\varepsilon \nabla P + \nabla \theta_p \frac{\partial P}{\partial \theta_p} \right) \cdot \mathbf{g} - \frac{1}{\mu} \varepsilon \nabla k \cdot \mathbf{g}$$
$$- \frac{k}{\mu} \left[\varepsilon \nabla \cdot \left(\varepsilon \nabla P + \nabla \theta_p \frac{\partial P}{\partial \theta_p} \right) + \nabla \theta_p \cdot \frac{\partial}{\partial \theta_p} \left(\varepsilon \nabla P + \nabla \theta_p \frac{\partial P}{\partial \theta_p} \right) \right]$$
$$= 0. \tag{B18}$$

Retaining only terms of order $\varepsilon^0 \sim 1$ results in

$$\alpha_p \frac{\partial \theta_p}{\partial t} \frac{\partial P}{\partial \theta_p} + \alpha_u \frac{\partial \mathbf{u}}{\partial \theta_u} \cdot \nabla \theta_u \frac{\partial \theta_p}{\partial t} \frac{\partial P}{\partial \theta_p} + \alpha \frac{\partial \theta_u}{\partial t} \frac{\partial^2 \mathbf{u}}{\partial \theta_u^2} \cdot \nabla \theta_u$$

$$- \beta_p \nabla \theta_p \cdot \nabla \theta_p \left(\frac{\partial P}{\partial \theta_p} \right)^2 - \gamma \nabla \theta_p \cdot \mathbf{g} \frac{\partial P}{\partial \theta_p} - \frac{k}{\mu} \nabla \theta_p \cdot \nabla \theta_p \frac{\partial^2 P}{\partial \theta_p^2} = 0.$$

$$(\text{B19})$$

Using the notation for the gradient vectors $\mathbf{p}$ and $\mathbf{s}$, as defined in (B11) and (B12), respectively, I can rewrite equation (B19) more compactly. Similarly, I can substitute $\bar{P}$ and $\bar{U}$ for the partial derivatives of P and $\mathbf{u}$ with respect to the phase variables θ_p and θ_u, as in equations (B13) and (B14). Thus, equation (B19) can be written as

$$\alpha_p \frac{\partial \theta_p}{\partial t} \bar{P} + \alpha_u \frac{\partial \theta_p}{\partial t} \mathbf{s} \cdot \bar{U} \bar{P} + \alpha \frac{\partial \theta_u}{\partial t} \mathbf{s} \cdot \bar{U}$$

$$- \beta_p p^2 \bar{P}^2 - \gamma \mathbf{p} \cdot \mathbf{g} \bar{P} - \frac{k}{\mu} p^2 \bar{P} = 0.$$

$$(\text{B20})$$

References

Aki, K., and P. G. Richards (1980), *Quantitative Seismology*, W. H. Freeman, San Francisco, Calif.

Anile, A. M., J. K. Hunter, P. Pantano, and G. Russo (1993), *Ray Methods for Nonlinear Waves in Fluids and Plasmas*, Longman, New York.

Bear, J. (1972), *Dynamics of Fluids in Porous Media*, Dover, New York.

Bemer, E., M. Bouteca, O. Vincke, N. Hoteit, and O. Ozanam (2001), Poromechanics: From linear to nonlinear poroelasticity and poroviscoelasticity, *Oil Gas Sci. Technol.*, *56*, 531–544.

Bertram, A. (2008), *Elasticity and Plasticity of Large Deformations*, Springer, Berlin.

Bethke, C. M., and T. F. Corbet (1988), Linear and nonlinear solutions for one-dimensional compaction flow in sedimentary basins, *Water Resour. Res.*, *24*, 461–467.

Biot, M. A. (1941), General theory of three-dimensional consolidation, *J. Appl. Phys.*, *12*, 155–164.

Biot, M. A. (1956a), Theory of propagation of elastic waves in a fluid-saturated porous solid. I. Low-frequency range, *J. Acoust. Soc. Am.*, *28*, 168–178.

Biot, M. A. (1956b), Theory of propagation of elastic waves in a fluid-saturated porous solid. II. Higher frequency range, *J. Acoust. Soc. Am.*, *28*, 179–191.

Biot, M. A. (1962), Mechanics of deformation and acoustic propagation in porous media, *J. Appl. Phys.*, *33*, 1482–1498.

Biot, M. A. (1973), Nonlinear and semilinear rheology of porous solids, *J. Geophys. Res.*, *78*, 4924–4937.

Biot, M. A., and D. G. Willis (1957), Elastic coefficients of the theory of consolidation, *J. Appl. Mech.*, *24*, 594–601.

Bracewell, R. N. (1978), *The Fourier Transform and Its Applications*, McGraw-Hill, New York.

Brillouin, L. (1964), *Tensors in Mechanics and Elasticity*, Academic, New York.

Burridge, R., and J. B. Keller (1981), Poroelasticity equations derived from microstructure, *J. Acoust. Soc. Am.*, *70*, 1140–1146.

Cappa, F., Y. Guglielmi, J. Rutqvist, C.-F. Tsang, and A. Thoraval (2006), Hydromechanical modelling of pulse tests that measure fluid pressure and fracture normal displacement at the Coaraze Laboratory site, France, *Int. J. Rock Mech. Min. Sci.*, *43*, 1062–1082, doi:10.1016/j.ijrmms.2006.03.006.

Cerveny, V. (1972), Seismic rays and ray intensities in inhomogeneous anisotropic media, *Geophys. J. R. Astron. Soc.*, *29*, 1–13.

Chapman, C. H. (2004), *Fundamentals of Seismic Wave Propagation*, Cambridge Univ. Press, Cambridge, U. K.

Cheng, A. H.-D., and Y. Abousleiman (2008), Intrinsic poroelasticity constants and a semilinear model, *Int. J. Numer. Anal. Methods Geomech.*, *32*, 803–831.

Cohen, J. K., and R. M. Lewis (1967), A ray method for the asymptotic solution of the diffusion equation, *J. Inst. Math. Appl.*, *3*, 266–290.

Courant, R., and D. Hilbert (1962), *Methods of Mathematical Physics*, Interscience, New York.

Cox, D., J. Little, and D. O'Shea (1998), *Using Algebraic Geometry*, Springer, New York.

Crandall, M. G., and P.-L. Lions (1983), Viscosity solutions of Hamilton-Jacobi equations, *Trans. Am. Math. Soc.*, *277*, 1–43.

Crandall, M. G., L. C. Evans, and P.-L. Lions (1984), Some properties of viscosity solutions of Hamilton-Jacobi equations, *Trans. Am. Math. Soc.*, *282*, 487–502.

Daley, T. M., M. A. Schoenberg, J. Rutqvist, and K. T. Nihei (2006), Fractured reservoir: An analysis of coupled elastodynamic and permeability changes from pore-pressure variations, *Geophysics*, *71*, O33–O41.

de Boer, R. (2000), *Theory of Porous Media*, Springer, Berlin.

de Marsily, G. (1986), *Quantitative Hydrogeology*, Academic, San Diego, Calif.

Eaton, D. W. S. (1993), Finite difference travel-time calculation for anisotropic media, *Geophys. J. Int.*, *114*, 273–280.

Ehlers, W. (1992), An elastoplasticity model in porous media theories, *Transp. Porous Media*, *9*, 49–59.

Eringen, A. C. (1962), *Nonlinear Theory of Continuous Media*, McGraw-Hill, New York.

Gobran, B. D., W. E. Brigham, and H. J. Ramey Jr. (1987), Absolute permeability as a function of confining pressure, pore pressure, and temperature, *SPE Form. Eval.*, March, 77–84.

Goddard, J. D. (1990), Nonlinear elasticity and pressure-dependent wave speeds in granular media, *Proc. R. Soc. London, Ser. A*, *430*, 105–131.

Goldenblat, I. I. (1962), *Some Problems of the Mechanics of Deformable Media*, P. Noordhoff, Groningen, Netherlands.

Iyer, H. M., and K. Hirahara (1993), *Seismic Tomography: Theory and Practice*, Chapman and Hall, London.

Jacob, C. E., and S. W. Lohman (1952), Non-steady flow to a well of constant drawdown in an extensive aquifer, *Eos Trans. AGU*, *33*, 559–569.

Jaeger, J. C., N. G. W. Cook, and R. W. Zimmerman (2007), *Fundamentals of Rock Mechanics*, Blackwell, Oxford, U. K.

Jaunzemis, W. (1967), *Continuum Mechanics*, Macmillan, New York.

Johnson, K. L. (1985), *Contact Mechanics*, Cambridge Univ. Press, Cambridge, U. K.

Karal, F. C., and J. B. Keller (1959), Elastic wave propagation in homogeneous and inhomogeneous media, *J. Acoust. Soc. Am.*, *31*, 694–705.

Kline, M., and I. W. Kay (1965), *Electromagnetic Theory and Geometrical Optics*, John Wiley, New York.

Kravtsov, Y. A., and Y. I. Orlov (1990), *Geometrical Optics of Inhomogeneous Media*, Springer, Berlin.

Lanczos, C. (1986), *The Variational Principles of Mechanics*, Dover, New York.

Lecomte, I. (1993), Finite difference calculation of first traveltimes in anisotropic media, *Geophys. J. Int.*, *113*, 318–342.

LeVeque, R. J. (1992), *Numerical Methods for Conservation Laws*, Birkhauser, Basel, Switzerland.

Levy, T. (1979), Propagation of waves in a fluid-saturated porous elastic solid, *Int. J. Eng. Sci.*, *17*, 1005–1014.

Lewis, R. W., and B. Schrefler (1978), A fully coupled consolidation model of the subsidence of Venice, *Water Resour. Res.*, *14*, 223–230.

Liu, H.-H., J. Rutqvist, and J. G. Berryman (2009), On the relationship between stress and elastic strain for porous and fractured rock, *Int. J. Rock Mech. Min. Sci.*, *46*, 289–296.

Luneburg, R. K. (1966), *Mathematical Theory of Optics*, Univ. of Calif. Press, Berkeley.

Makse, H. A., N. Gland, D. L. Johnson, and L. Schwartz (2004), Granular packings: Nonlinear elasticity, sound propagation, and collective relaxation dynamics, *Phys. Rev. E*, *70*, 1–19.

Menke, W. (1984), *Geophysical Data Analysis: Discrete Inverse Theory*, Academic, Orlando, Fla.

Mindlin, R. D. (1949), Compliance of elastic bodies in contact, *J. Appl. Mech.*, *71*, 259–268.

Morland, L. W. (1972), A simple constitutive theory for a fluid-saturated porous solid, *J. Geophys. Res.*, *77*, 890–900.

Murnaghan, F. D. (1951), *Finite Deformation of an Elastic Solid*, John Wiley, New York.

Murphy, W., C. Huang, Z. Dash, G. Zyvoloski, and A. White (2004), Semianalytical solutions for fluid flow in rock joints with pressure-dependent openings, *Water Resour. Res.*, *40*, W12506, doi:10.1029/2004WR 003005.

Nelson, I., and M. L. Baron (1971), Application of variable moduli models to soil behavior, *Int. J. Solid Struct.*, *7*, 399–417.

Noble, B., and J. W. Daniel (1977), *Applied Linear Algebra*, Prentice-Hall, Englewood Cliffs, N. J.

Noorishad, J., C. F. Tsang, and P. A. Witherspoon (1984), Coupled thermal-hydraulic-mechanical phenomena in saturated fractured porous rocks: Numerical approach, *Water Resour. Res.*, *89*, 10,365–10,373.

Ogden, R. W. (1984), *Non-Linear Elastic Deformations*, John Wiley, New York.

Press, W. H., S. A. Teukolsky, W. T. Vetterling, and B. P. Flannery (1992), *Numerical Recipes*, Cambridge Univ. Press, Cambridge, U. K.

Pride, S. R. (2005), Relationships between seismic and hydrological properties, in *Hydrogeophysics*, pp. 253–291, Springer, New York.

Raghavan, R., D. T. Scorer, and F. G. Miller (1972), An investigation by numerical methods of the effect of pressure-dependent rock and fluid properties, *Soc. Pet. Eng. J.*, *12*, 267–276.

Roddeman, D. G. (2001), TOCHNOG users manual: A free explicit/implicit finite element program, *FEAT Rep. 177*, Finite Element Appl. Technol., Heerlen, Netherlands. [Available at http://www.feat.nl.]

Rucci, A., D. W. Vasco, and F. Novali (2010), Fluid pressure arrival time tomography: Estimation and assessment in the presence of inequality constraints, with an application to a producing gas field at Krechba, Algeria, *Geophysics*, *75*, O39–O55.

Rutqvist, J., J. Noorishad, and C.-F. Tsang (1998), Determination of fracture storativity in hard rocks using high-pressure injection testing, *Water Resour. Res.*, *34*, 2551–2560.

Samaniego, V. F., W. E. Brigham, and F. G. Miller (1977), An investigation of transient flow of reservoir fluids considering pressure-dependent rock and fluid properties, *Soc. Pet. Eng. J.*, *17*, 140–149.

Segall, P. (1985), Stress and subsidence resulting from subsurface fluid withdrawal in the epicentral region of the 1983 Coalinga earthquake, *J. Geophys. Res.*, *90*, 6801–6816.

Sethian, J. A. (1990), Numerical algorithms for propagating interfaces: Hamilton-Jacobi equations and conservation laws, *J. Differ. Geom.*, *31*, 131–161.

Sethian, J. A. (1999), *Level Set Methods*, Cambridge Univ. Press, Cambridge, U. K.

Sethian, J. A., and J. D. Strain (1992), Crystal growth and dendritic solidification, *J. Comput. Phys.*, *98*, 231–253.

Shapiro, S. A. (2003), Piezosensitivity of porous and fractured rocks, *Geophysics*, *68*, 482–486.

Shen, M. C. (1983), Ray method for flow of a compressible viscous fluid, *SIAM J. Appl. Math.*, *43*, 822–833.

Sneddon, I. N. (2006), *Elements of Partial Differential Equations*, Dover, New York.

Soukina, S. M., D. Gajewski, and B. M. Kashtan (2003), Traveltime computation for 3D anisotropic media by a finite-difference perturbation method, *Geophys. Prospect.*, *51*, 431–441.

Sturmfels, B. (2002), *Solving Systems of Polynomial Equations*, Am. Math. Soc., Providence, R. I.

Terzaghi, K. (1943), *Theoretical Soil Mechanics*, John Wiley, New York.

Theis, C. V. (1935), The relation between the lowering of the piezometric surface and the rate and duration of discharge of a well using groundwater storage, *Eos Trans. AGU*, *16*, 519–524.

Truesdell, C., and W. Noll (1965), The non-linear field theories of mechanics, in *Encyclopedia of Physics*, edited by S. Flugge, 591 pp., Springer, Berlin.

Vasco, D. W. (2008), Modelling quasi-static poroelastic propagation using an asymptotic approach, *Geophys. J. Int.*, *173*, 1119–1135, doi:10.1111/j.1365-246X.2009.03758.

Vasco, D. W. (2009), Modelling broad-band poroelastic propagation using an asymptotic approach, *Geophys. J. Int.*, *179*, 299–318, doi:10.1111/j.1365-246X.2009.04263.

Vasco, D. W. (2010), On fluid flow in a heterogeneous medium under nonisothermal conditions, *Water Resour. Res.*, *46*, W12513, doi:10.1029/2010WR009571.

Vasco, D. W. (2011), On the propagation of a coupled saturation and pressure front, *Water Resour. Res.*, *47*, W03526, doi:10.1029/2010WR009740.

Vasco, D. W., and S. Finsterle (2004), Numerical trajectory calculations for the efficient inversion of flow and tracer observations, *Water Resour. Res.*, *40*, W01507, doi:10.1029/2003WR002362.

Vasco, D. W., and S. Minkoff (2009), Modelling flow in a pressure-sensitive, heterogeneous medium, *Geophys. J. Int.*, *179*, 972–989.

Vasco, D. W., H. Keers, and K. Karasaki (2000), Estimation of reservoir properties using transient pressure data: An asymptotic approach, *Water Resour. Res.*, *36*, 3447–3465.

Vasco, D. W., H. Keers, J. E. Peterson, and E. Majer (2003), Zeroth-order asymptotics: Waveform inversion of the lowest degree, *Geophysics*, *68*, 614–628.

Vidale, J. (1988), Finite-difference calculation of travel times, *Bull. Seismol. Soc. Am.*, *78*, 2062–2076.

Virieux, J., C. Flores-Luna, and D. Gibert (1994), Asymptotic theory for diffusive electromagnetic imaging, *Geophys. J. Int.*, *119*, 857–868.

Walsh, J. B., and W. F. Brace (1984), The effect of pressure on the transport properties of rock, *J. Geophys. Res.*, *89*, 9425–9431.

Wang, H. F. (2000), *Theory of Linear Poroelasticity*, Princeton Univ. Press, Princeton, N. J.

Whitham, G. B. (1974), *Linear and Nonlinear Waves*, John Wiley, New York.

Witherspoon, P. A., J. S. Y. Wang, K. Iwai, and J. E. Gale (1980), Validity of cubic law for fluid flow in a deformable rock fracture, *Water Resour. Res.*, *16*, 1016–1024.

Wu, Y.-S., and K. Pruess (2000), Integral solutions for transient fluid flow through a porous medium with pressure-dependent permeability, *Int. J. Rock Mech. Min. Sci.*, *37*, 51–61.

Zimmerman, R. W. (1991), *Compressibility of Sandstones*, Elsevier, New York.

D. W. Vasco, Earth Sciences Division, Lawrence Berkeley National Laboratory, Bldg. 64, 1 Cyclotron Rd., Berkeley, CA 94720, USA. (dwvasco@lbl.gov)